EG&G Idaho Inc

FORM EG&G 229
Rev 01-80

LOFT TECHNICAL REPORT

Title Pitot Tube Performance in Transient Steam-Water Flow	LTR No. LO-87-80-142
Author Richard R. Good	Released By LOFT CDCS
Performing Organization LOFT Measurements Division	Date January 29, 1981
LOFT Review and Approval	Project System Engineer

MD Mgr. LTSD Acting Mgr.

ABSTRACT

Performance of pitot tube rakes during a series of transient two-phase flow tests is evaluated. The flow conditions during the test closely mapped those measured in the Loss-of-Fluid Test (LOFT) reactor system. The performance of the pitot tubes is evaluated by comparing the mass flow calculated using the momentum flux derived by the pitot tubes and the mass flow from the reference weigh system. The pitot tubes performed satisfactorily, but quantifiable assessments of the effect of Kiel shield, pitot rake cooling, and pitot rake purging were not possible.

DISPOSITION OF RECOMMENDATIONS

No disposition required.

SUMMARY

The performance of two configurations of pitot tube rakes were evaluated in transient two-phase flow. The flow fields were designed to simulate those found in the Loss-of-Fluid Test (LOFT) reactor primary coolant piping during a large LOCE. The flow fields were simulated by duplicating the LOFT piping geometry. Instrumentation was provided to measure pressure, temperature, fluid density, pipe differential pressures, and global mass flow. The experimental instrumentation consisted of two rakes of pitot tubes. One rake consisting of five unshielded pitot tubes and one rake of four Kiel shielded pitot tubes. The performance of the pitot tube rakes was evaluated by comparing the mass flow calculated using the pitot tube rakes as momentum flux meters and the density measured by the six-beam gamma densitometer, and the mass flow from the reference load cell system. Attempts to quantify the effects of Kiel shields, continuous cooling of the pilot tube rakes, and purge of the pitot tube rakes were unsuccessful. The pitot rakes performed well with an uncertainty of -3.77 %RG. The range of difference between reference mass flow and pitot tube rake measured mass flow was +19.66 %RG and -9.48 %RG.

CONTENTS

FIGURES

TABLES

PITOT TUBE PERFORMANCE IN TRANSIENT STEAM-WATER FLOW

1. INTRODUCTION

Pitot tubes are used to measure the momentum flux (Mg/ms^2) of a fluid. They are invasive devices that depend on sensing the differential pressure between two pressure taps: one of these taps is normal to the flow (the dynamic tap), and one is parallel to the flow (the static tap). The reduction of the resulting differential pressure to momentum flux when the fluid is single phase is a well understood process;[1] however, when the fluid was multiphase, the dependence of differential pressure on momentum flux still remained to be fully quantified. This is the subject of this pitot tube performance evaluation.

Data for this pitot tube performance evaluation were obtained from transient two-phase flow tests conducted to provide data for calibration and model development of instruments used in the Loss-of-Fluid Test (LOFT) facility. Consequently, the transient tests were designed to replicate those conditions found within the LOFT[2] primary coolant piping during a LOFT large break (double-ended offset shear of a primary coolant pipe) experiment. The transient tests were performed at the LOFT Transient Calibration Facility (LTCF)[3] while it was located at Wyle Labs in Norco, California. The tests were initiated from 15.5 MPa and 550 K. The duration for each test was between 60 and 150 s, depending on the size of the break being modeled.

A total of 11 tests were performed, including replications. Table 1 lists the tests and the corresponding system configuration. These tests provided data used to quantify the effects of water cooling, water purge, Kiel shields, piping geometry, and transient two-phase flow on pitot tube performance. These effects were determined by comparison of calculated mass flow using data from the pitot tubes and the reference mass flow derived from a set of load cells.[4]

The system reference instrumentation consisted of absolute pressure, temperature, density, and mass flow. Pressure and temperature were measured with force balance transducers and Type K, grounded junction

TABLE 1. TEST CONDITIONS

Test	Initial Temperature (K)	Initial Pressure (MPa)	Rake Type	Elbow	Orifice Size (in.)
IB2SP01	302	15.63	P	No	2
IB201	561	15.72	P	No	6
IA201	559	15.67	P	Yes	6
IA202	564	15.09	P	Yes	6
IIA201	564	15.511	P	Yes	2
IIA202	566	15.47	P	Yes	2
IIIA101	564	15.51	E	Yes	4
IIIA102	564	15.45	E	Yes	4
IIIA201	562	15.48	E	Yes	4
IIIA202	565	15.51	E	Yes	4
IVA101	565	15.46	E	Yes	2

thermocouples, respectively. Density was determined using a six-beam gamma densitometer. Reference mass flow was computed from the time derivative of the sum of the output of the load cells. Figure 1 is a diagram of the test facility, and Figures 2 through 5 are schematics of the instrument locations for each different test configuration.

The experimental instrumentation of interest to this report consisted of two pitot tube rakes. One pitot tube rake, the PDTT rake, was designed to fit in the port normally occupied by the drag disc-turbine rake. The PDTT consisted of five pitot tubes. The second pitot tube rake, the PECC rake, consisted of eight pitot tubes each equipped with a Kiel[5] shield and four thermocouples. Only four of the eight probes were used, as no reverse flow was expected to occur.

The results of the testing indicated that pitot tubes functioned well in a two-phase flow environment. However, the effects of the water purge, Kiel shields, and piping geometry on pitot tube performance were not well quantified with the limited data available.

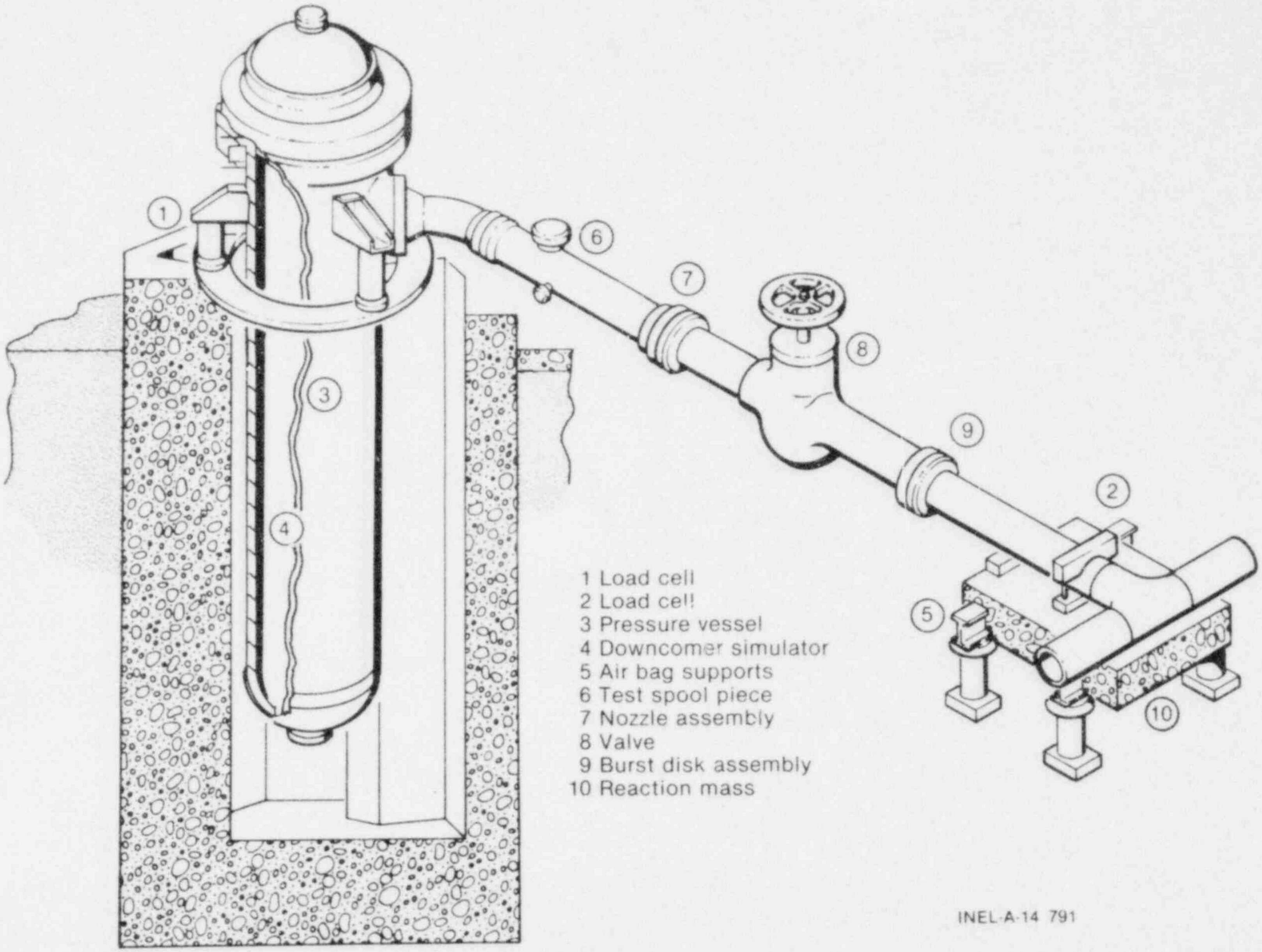

Figure 1. Schematic of the transient test facility.

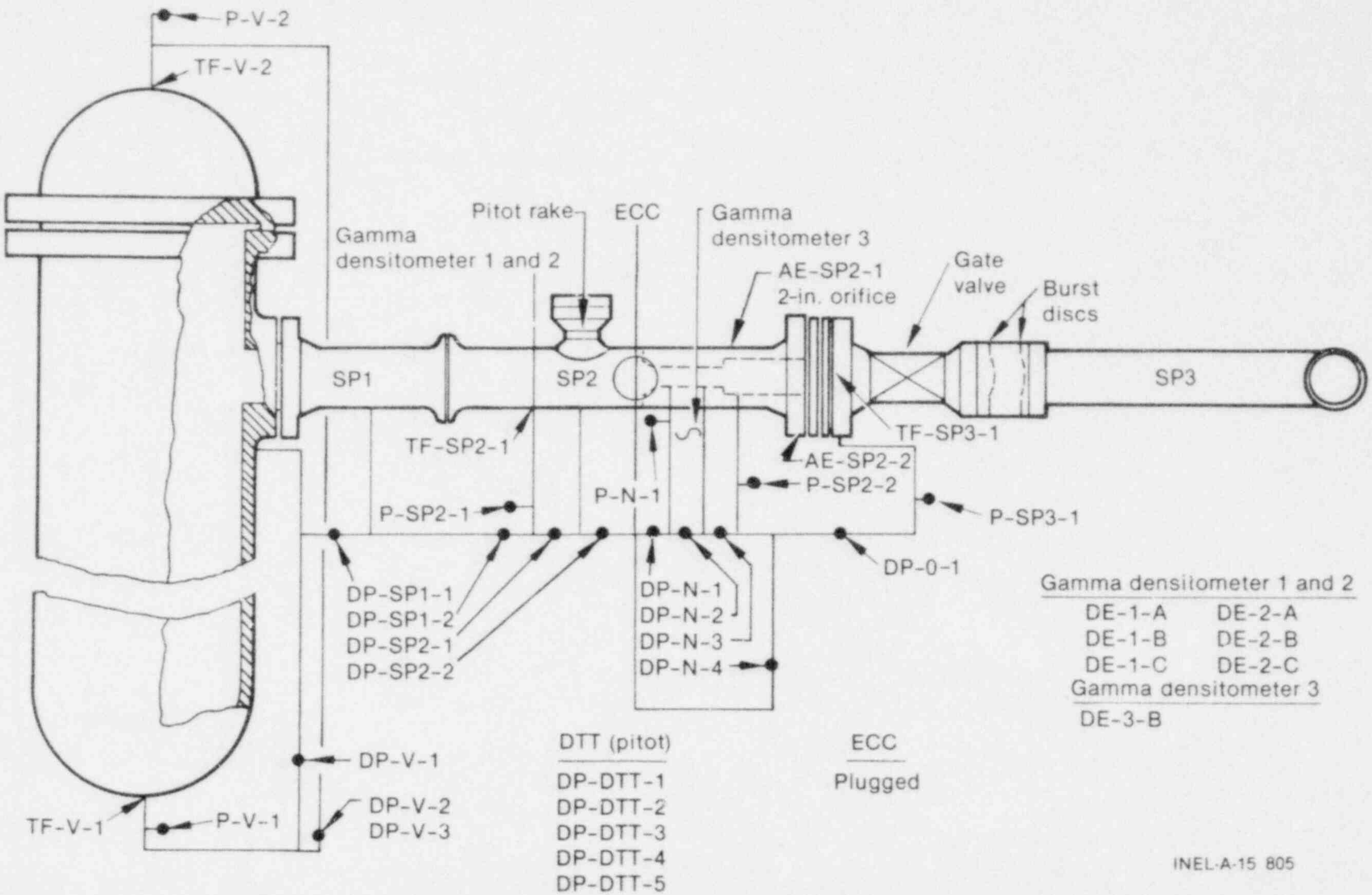

Figure 2. Test vessel, piping, and instrumentation schematic for Tests IA201, IA202, IB201, and IB2SP01.

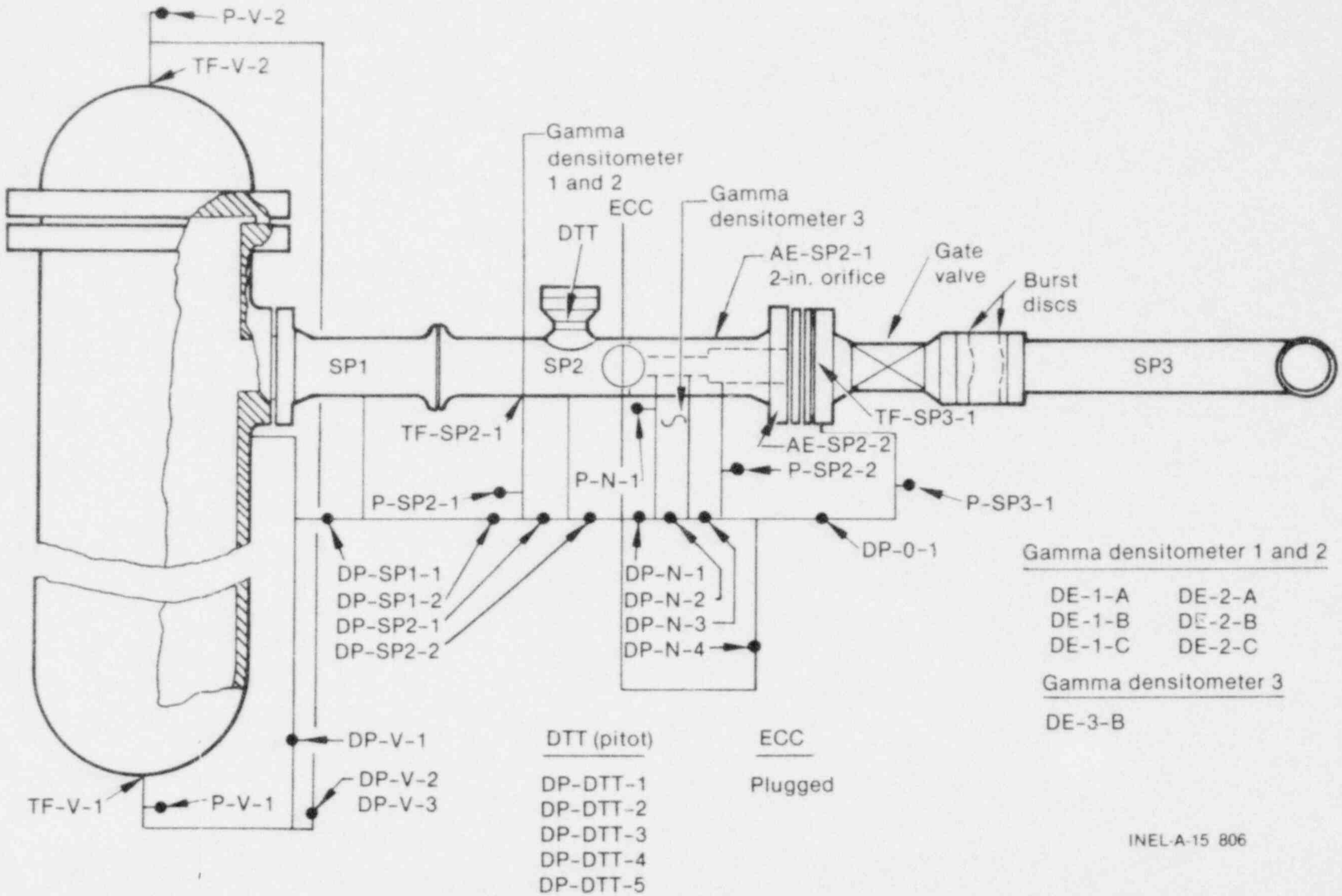

Figure 3. Test vessel, piping, and instrumentation schematic for Tests IIA201 and IIA202.

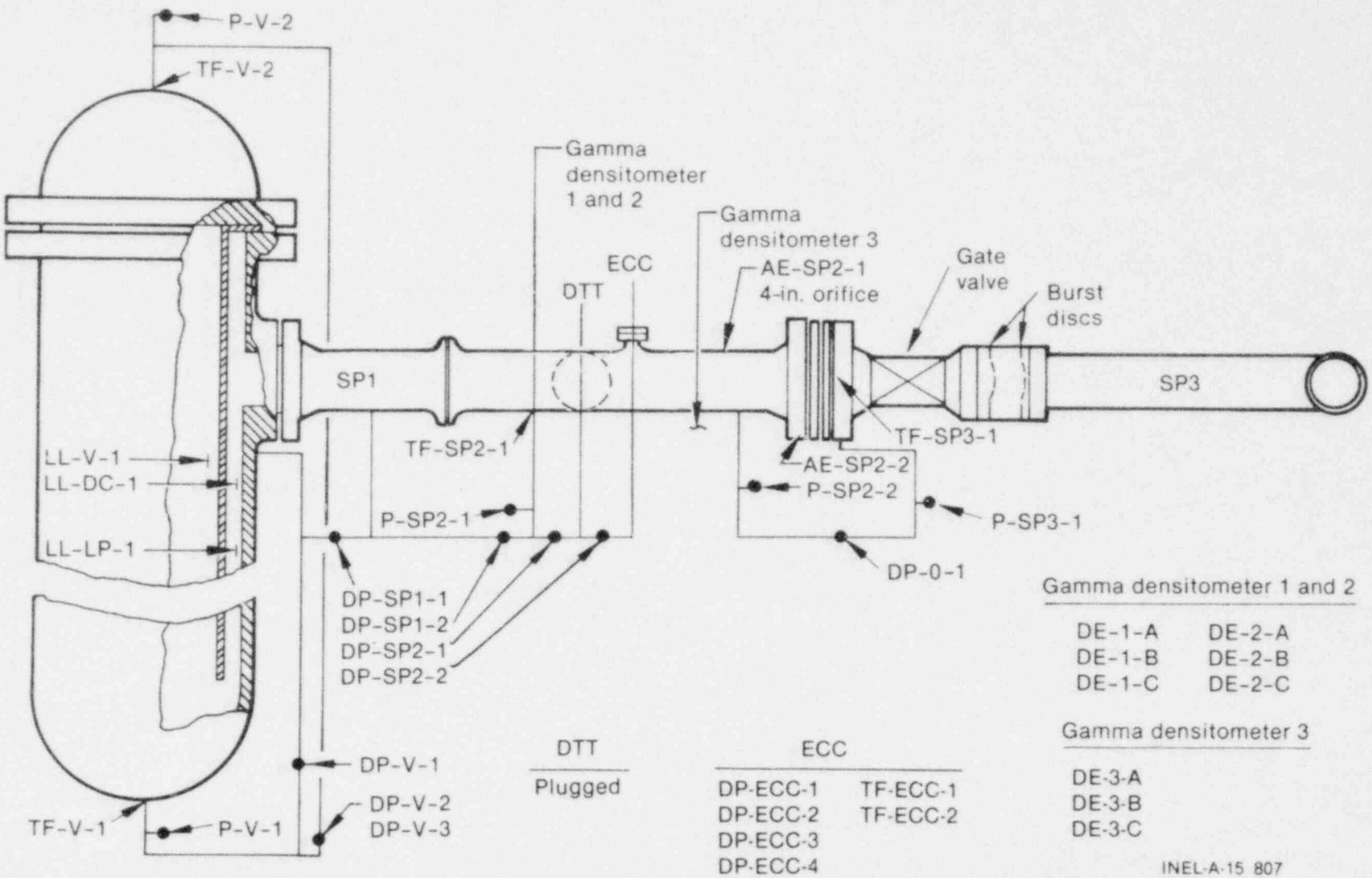

Figure 4. Test vessel, piping, and instrumentation schematic for Tests IIIA101, IIIA102, IIIA201, and IIIA202.

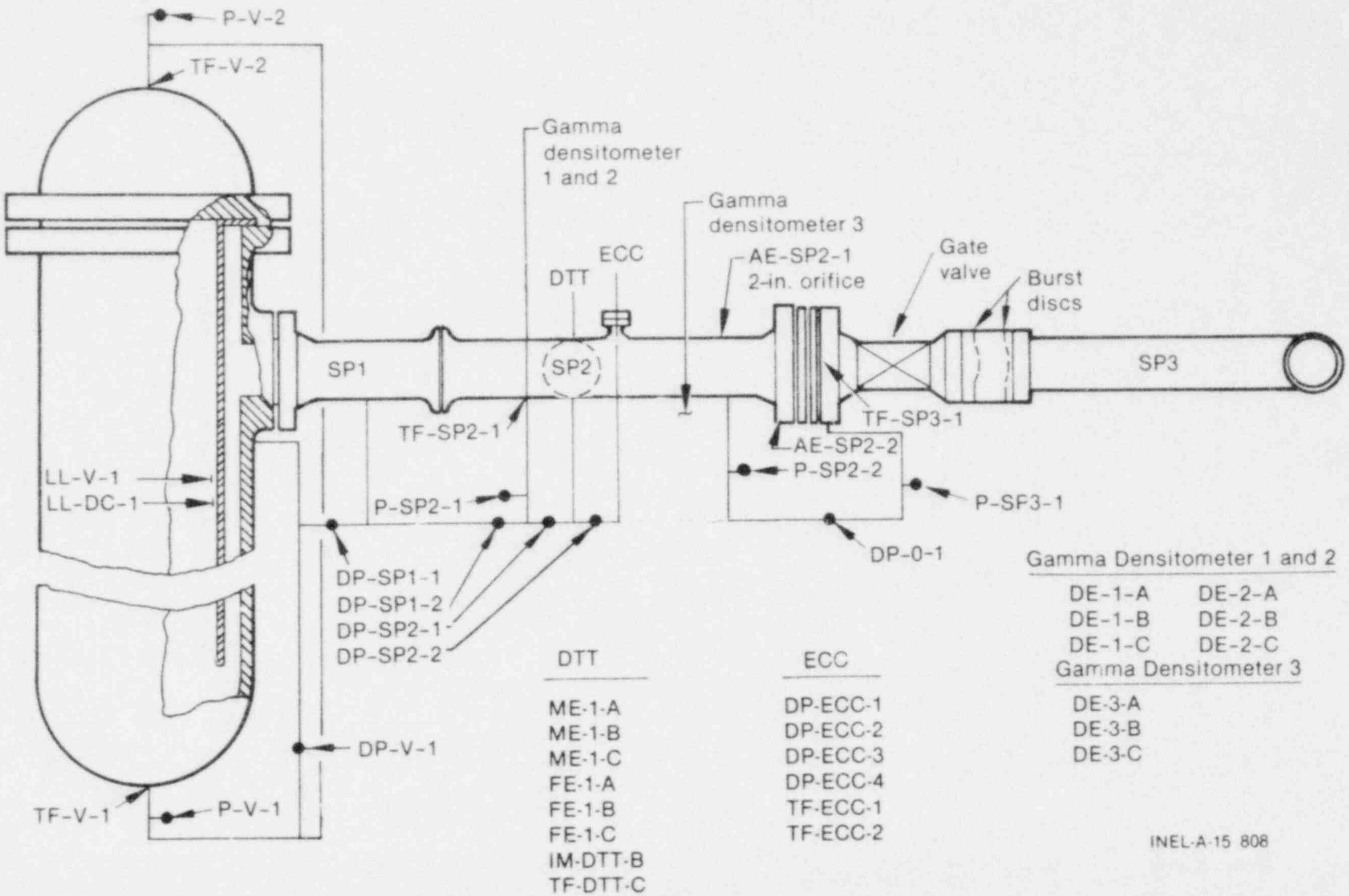

Figure 5. Test vessel, piping, and instrumentation schematic for Tests IVA101 and IVA102.

LTR LO-87-80-142

2. TEST FACILITY DESCRIPTION

The LTCF was designed to replicate flow conditions existing within LOFT primary cooling piping during a loss-of-coolant experiment (LOCE). A LOCE results from a breach in the primary coolant boundary and the subsequent loss of coolant. All large break (double-ended offset shear) LOCEs (which are the only type investigated in this report) result in a rapid depressurization of the system and, consequently, a mixture of steam-water flowing throughout the system. Flowing mixtures of steam-water result in very complicated mass and velocity profiles. These profiles are affected by the system temperature, pressure, and geometry; hence, replication of LOFT fluid conditions required exact duplication of the LOFT reactor facility's geometry, pressure, and temperature.

All pre-LOCE conditions for the transient two-phase flow tests were patterned after those common to LOFT (nominal temperature and pressure of 555 K and 15.5 MPa, respectively, with the vessel full of water). Actual test conditions are given in Table 1. In general, the initial conditions were close to nominal with a mean pressure of 15.49 MPa and a mean temperature of 563.4, and in all tests, the vessel was full (approximately 5.66 m^3) of water. These nominal conditions result in fluid velocities as high as 50 m/s and momentum fluxes of 100 Mg/ms^2 in the LOFT system.

The piping geometry upstream of the test section was changed several times during the testing. Figures 6 and 7 show the various piping geometries employed. The upstream piping was designed to simulate piping geometry variations upstream of equivalent measurement locations in LOFT. The upstream geometry variations included straight pipe and a 45-degree elbow. The facility was also operated with and without the pressure vessel flow skirt installed.

The general test procedure was designed to simulate a LOFT blowdown. Initial test conditions within the vessel varied from the nominal conditions by +0.2 and -0.1 MPa and +9 and -0 K. The blowdowns were initiated via a burst disc assembly located downstream of orifice. Digital and analog data were recorded for all tests. The digital data were prefiltered with an analog four-pole, 10-Hz filter and recor[illegible]) samples/second.

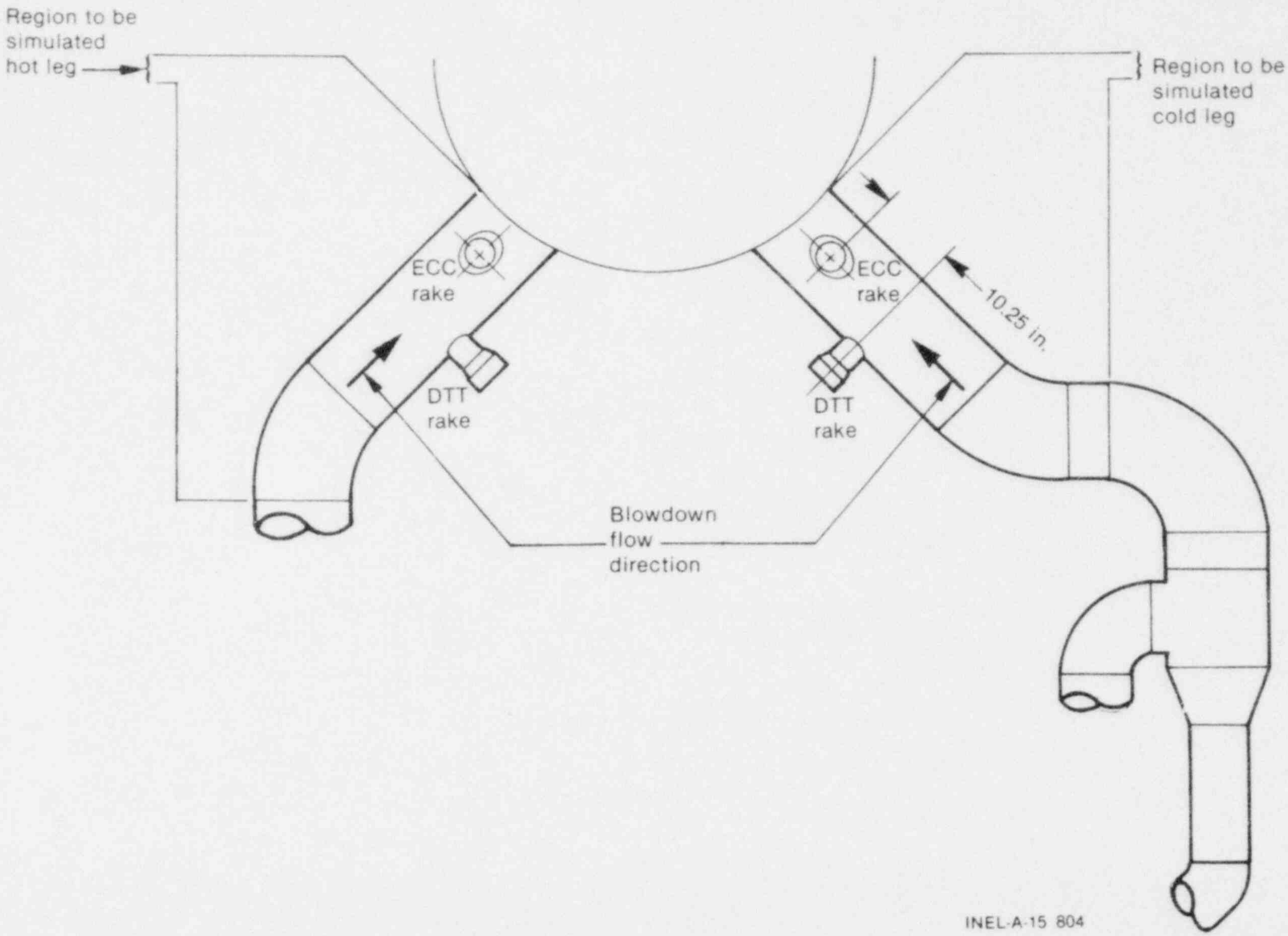

Figure 6. Intact loop piping layout.

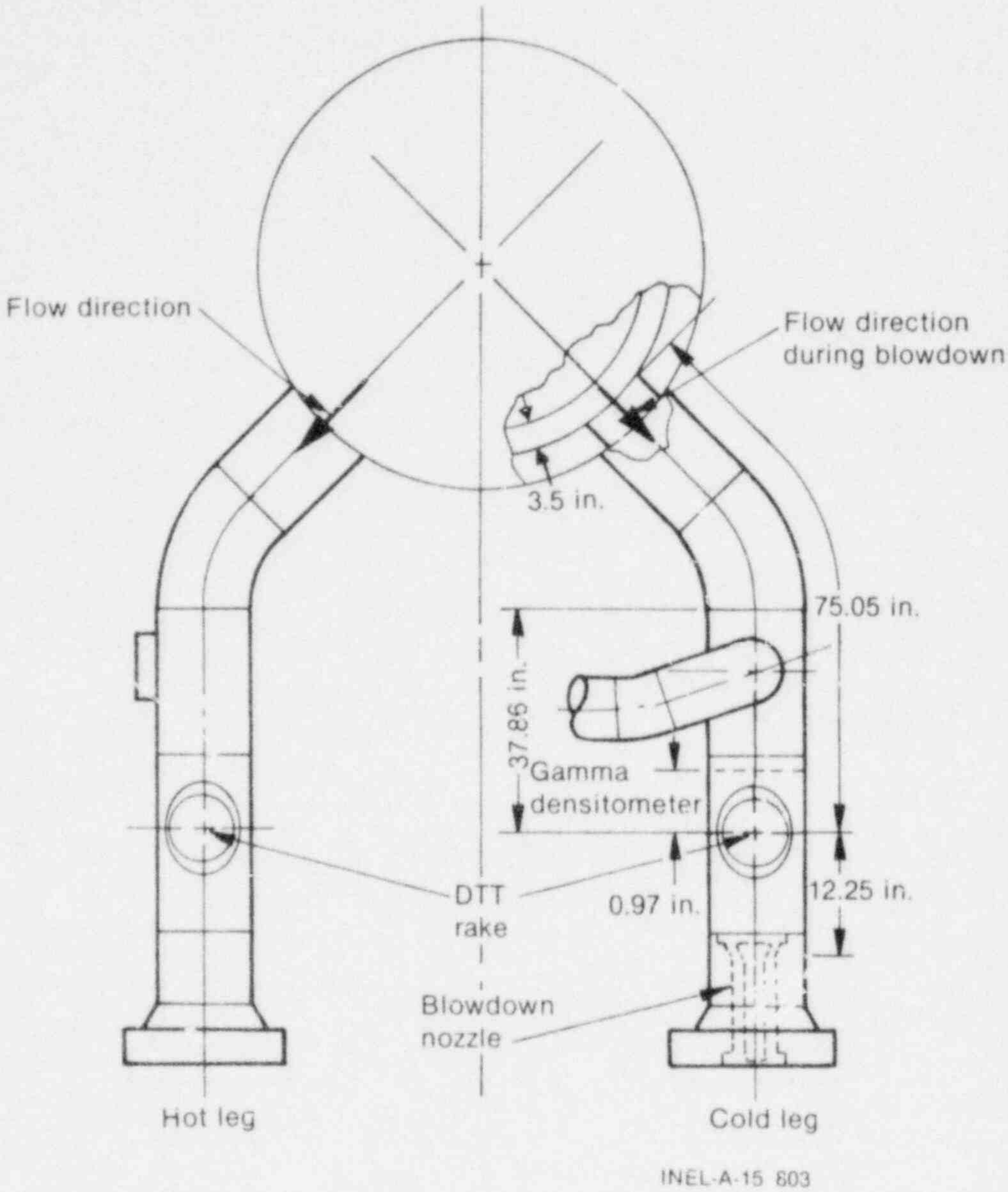

Figure 7. Broken loop piping layout.

Approximately 40 channels of digital data were recorded. The digital data were backed up with analog recorded data. The analog recordings were frequency modulated, having a frequency range of 0 to 5000 Hz (no prefiltering was applied to the analog data).

Voltage calibration steps were recorded both prior to and after each blowdown. In-place calibrations of all absolute pressure transducers were performed periodically; simultaneously, the pitot tube differential pressure cells line pressure sensitivity was quantified. Reference 3 provides a detailed description of the test setup and procedure.

The tests conducted with pitot tubes installed as the primary mass flow instrumentation served a twofold purpose: (a) to quantify the mass flow measuring capability of the pitot tubes when used in conjunction with a density measurement during two-phase flow, and (b) to quantify the effectiveness and effects of continuous purge systems for pitot tubes. Table 2 shows the test matrix used to accomplish these goals. Tests were conducted with equivalent geometries, but with and without purge water to the pitot tube rake. All tests were used to quantify the effectiveness of the pitot tube as a mass flow measuring device. The effects of purge water were monitored on two pairs of tests. Additionally, a series of tests was conducted with a pitot rake having Kiel shields, thus data to quantify the effects of Kiel shields were produced.

TABLE 2. TEST INSTRUMENTATION STATUS

Test	Instrument	Orientation	Purge	Cooling
IB2SP01	PDTT[a]	Vertical	On	On
IB201	PDTT	Vertical	On	On
IA201	PDTT	Vertical	Off	On
IA202	PDTT	Vertical	On	On
IIA201	PDTT	Vertical	On	On
IIA202	PDTT	Vertical	On	On
IIIA101	PECC[b]	Vertical	On	On
IIIA102	PECC	Vertical	On	On
IIIA201	PECC	Vertical	Off	On
IIIA202	PECC	Vertical	On	On
IVA101	PECC	Vertical	On	On

a. PDTT--LOFT test pitot tube rake.

b. PECC--LOFT ECC thermocouple pitot tube rake.

3. INSTRUMENTATION

EG&G Idaho, Inc., was responsible for both the test and reference instrumentation at the LTCF. The reference measurements included mass flow, pressure, temperature, and density. The mass flow and density measurement systems were designed by EG&G Idaho, Inc. Test instrumentation for the pitot tube tests consisted of two rakes of pitot tubes, one with and one without Kiel shields. The balance of the test and reference instrumentation were standard pressure, differential pressure, and temperature measuring instruments. Schematics of test instrumentation are shown in Figures 2, 3, 4, and 5.

The two pitot tube rakes (PDTT and PECC rakes) had substantially different design criteria. The PDTT rake was designed to measure the momentum flux profile at an instrument port where a rake of drag disc-turbines would be installed in other tests. The PDTT rake was to provide information to aid in the understanding of the performance of the drag disc-turbine rake. The second pitot tube rake, the PECC rake, was designed to measure the momentum flux profile at the point of emergency core coolant (ECC) injection in the LOFT reactor system. Figures 8 and 9 show the PDTT and PECC rakes. Figure 10 shows the test spool piece in which the rakes were installed. The primary design differences are the number of pitot probes and the use of Kiel shields. The PECC rake was required to measure a much more complex flow; hence, provision was made to measure both forward and reverse flow and to minimize the effect of nonaxial flows. Thus, each of the eight pitot tubes of the PECC rake was equipped with a Kiel shield; four faced upstream and four faced downstream. The PDTT rake was designed to measure unidirectional flows with little or no swirl component; hence, the PDTT has five pitot tubes without Kiel shields, spaced to cover equal areas.

The PECC and PDTT rakes did have some common design features. Both rakes were equipped with a purge system, used a static wall tap, and had a cooling system for the pitot tubes dynamic sense lines. The purge and cooling systems served a common purpose of keeping the dynamic sense lines full of water throughout a blowdown. The purge system (shown in Figure 11) was to maintain a small constant purge of water through each sense line. The transducer measurements were isolated from each other by the large (4.6 MPa)

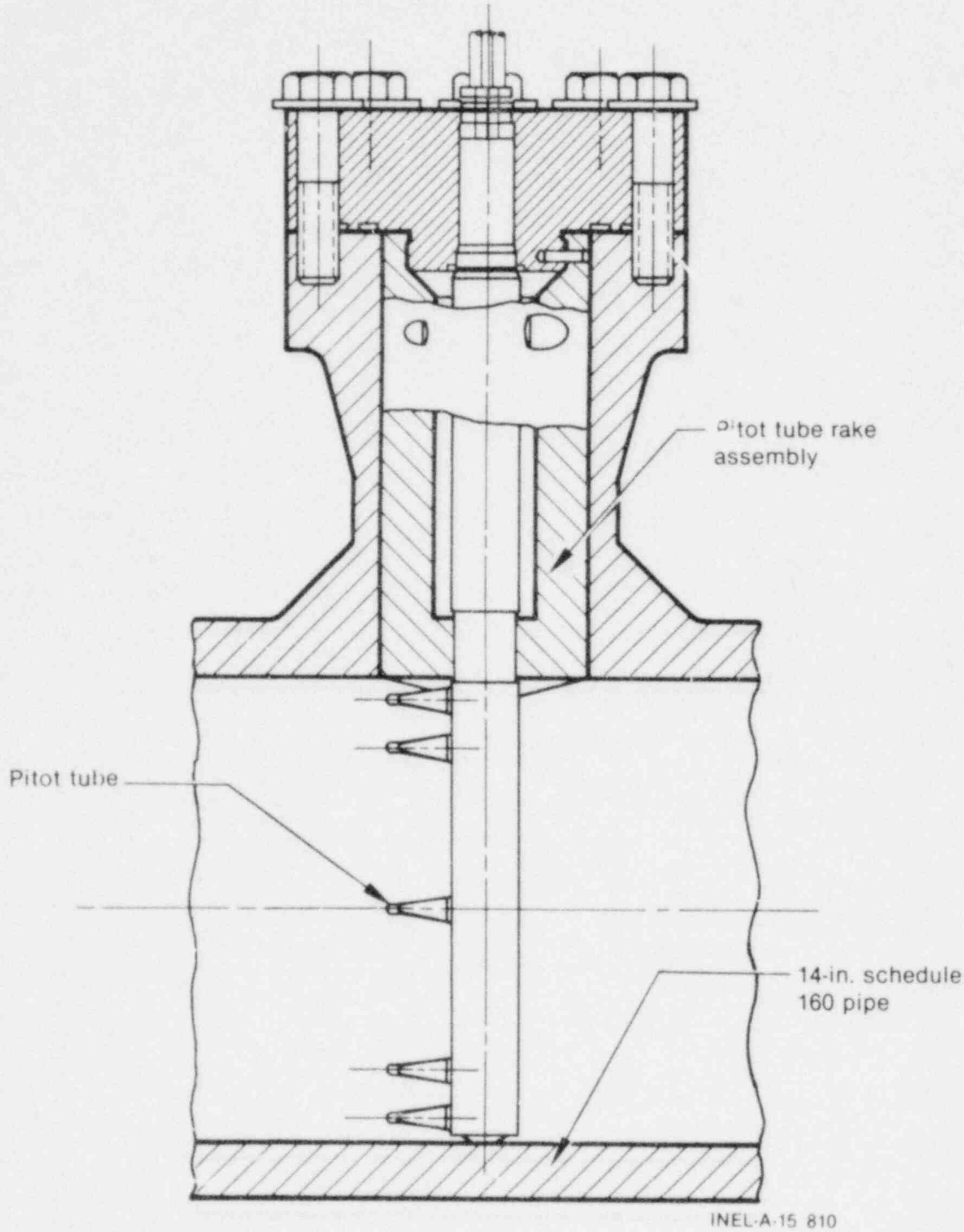

Figure 8. PDTT rake.

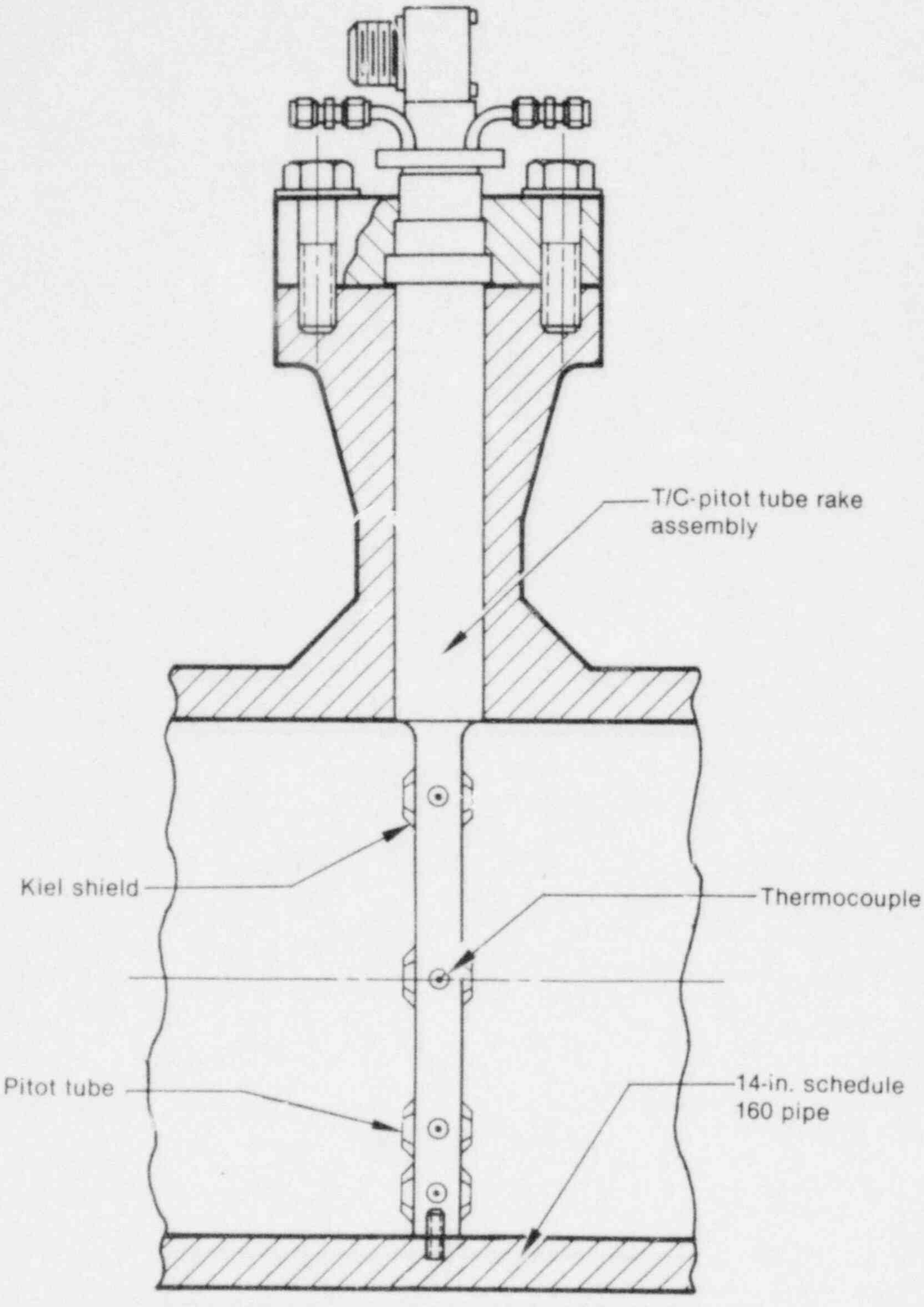

Figure 9. PECC rake.

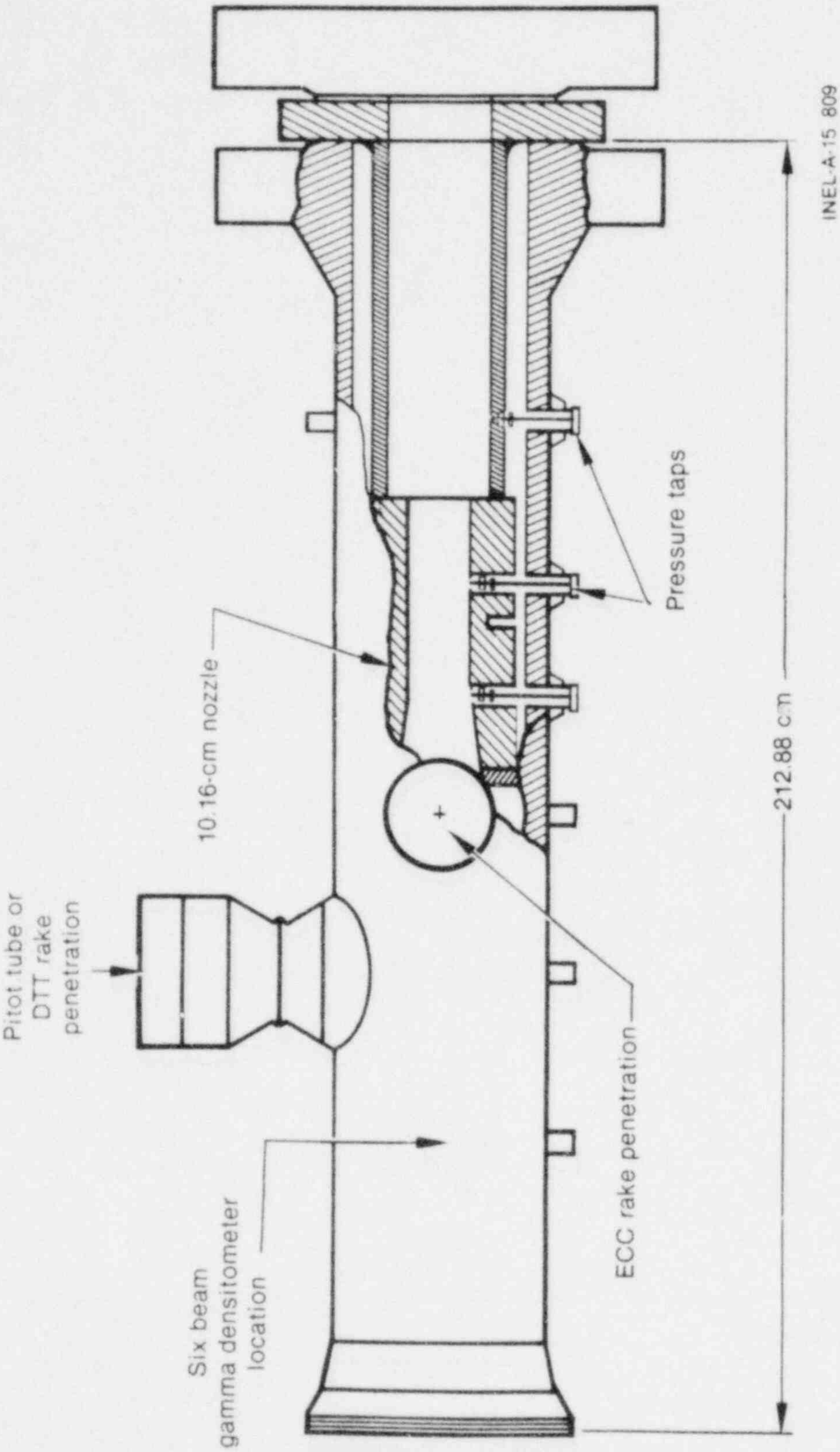

Figure 10. Schematic of transient test spool piece.

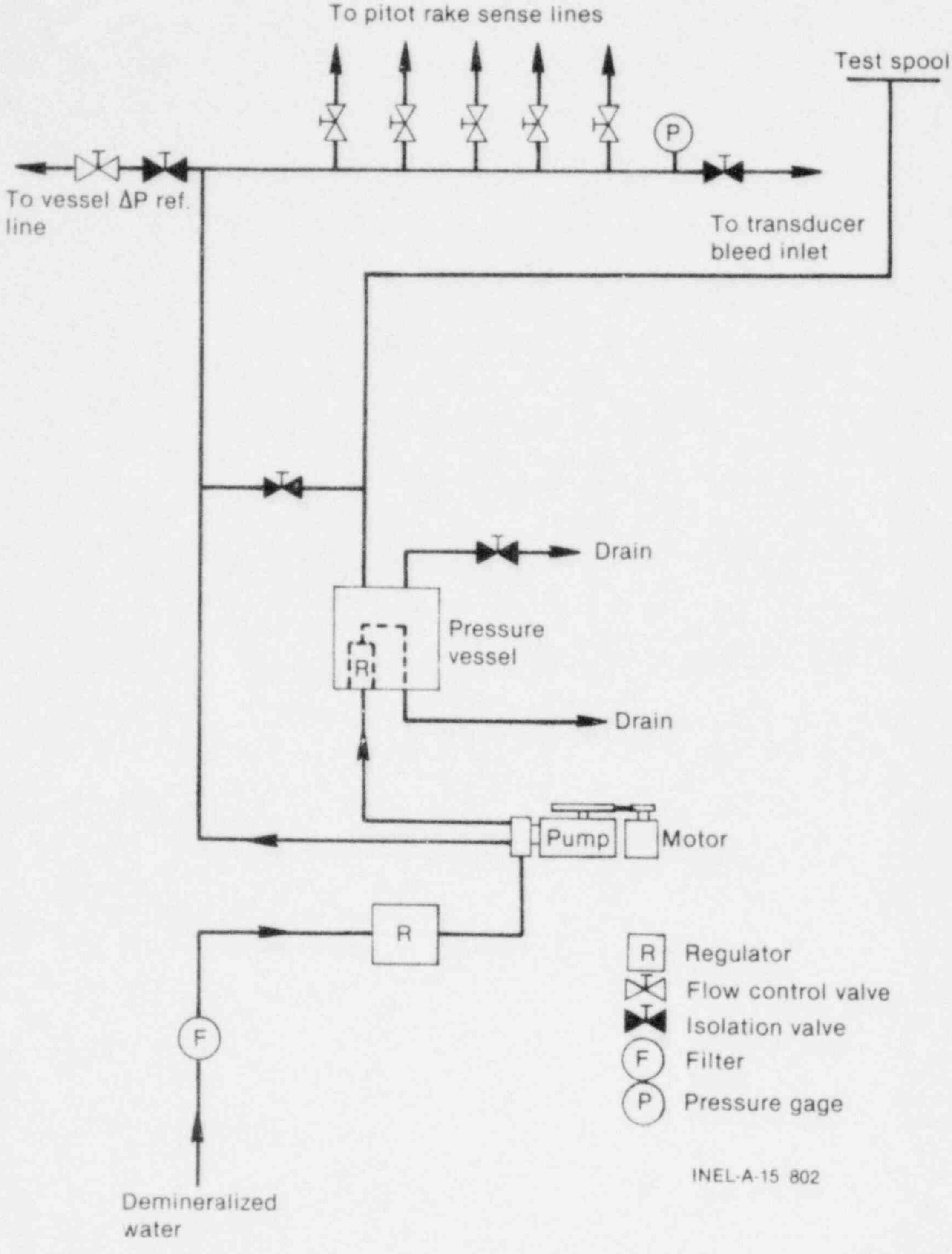

Figure 11. Schematic of continuous purge system.

pressure drop across the flow control valves sh n in Figure 11. The flow was to remain constant, as it was delivered under a constant head regardless of system pressure, and the water source was a positive displacement pump. The cooling system was designed to maintain the water in the sense lines subcooled during blowdowns. It was postulated that the cooling system might be sufficient to maintain the integrity of the sense lines alone; thus, some tests were performed with only the cooling system operational to test this hypo esis.

4. DATA REDUCTION EQUATIONS

The use of pitot tubes in single-phase fluids as momentum flux measuring devices has been well proven. The standard data reduction equation for single-phase flows is:

$$DP = 1/2 \cdot \rho \cdot V^2 \qquad (1)$$

or in the current case:

$$\rho V^2 = 2 \cdot DP \qquad (2)$$

where

DP = differential pressure

ρ = fluid density

V = fluid velocity.

Variations of Equation (1) have been suggested by many researchers to accommodate multiphase flows. The most successful variation to date is:

$$DP = (1/2) \cdot \gamma \cdot \rho_c \cdot V_c^2 + \beta(1 - \gamma) \cdot \rho_e \cdot V_e^2 \qquad (3)$$

where

DP and V are defined for Equation (1)

e = entrained phase

c = continuous phase

β = momentum transfer function = 0.5 for liquid continuous phase
= 1.0 for liquid entrained phase

$$\gamma = 1 - \left(\frac{\rho_m - \rho_l}{\rho_g - \rho_l}\right) = \text{void fraction} \quad (4)$$

ρ = density

m = mixture

l = liquid

g = gas.

Equation (3), developed by Anderson and Mantzournis,[5] unfortunately relies on the judgement of the analyst to decide what constitutes an adequate criteria for assigning the entrained phase to water or gas. The most popular criterion is void fraction. Anderson and Mantzournis have suggested a transition region of 0.7 void fraction for air-water flows. More recently, Fincke and Deason[1] found acceptable results for air-water flows with a transition between entrained phases occurring at 0.9 void fraction. Initial estimates for momentum flux were calculated using a transition of 0.9; this proved acceptable for all tests.

Pipe average mass flow was calculated by integrating the product of a density profile and a momentum flux profile as follows:

$$\dot{m} = A \int P(r)\, m(r)\, dr \quad (5)$$

where

P(r) = density as a function of radius

m(r) = momentum flux as a function of radius

A = area

$\dot{m}$ = mass flow.

The momentum flux profile was obtained from the pitot tube rake, and the density profile from the six-beam gamma densitometer. The exact procedure used for calculating the density and momentum flux profiles is documented in Reference 4. The density profile is computed by performing a least squares fit to a number of expected profiles. The best fit is then assumed to be the real profile. Density profiles used in this analysis were homogeneous, stratified, tilted stratified, annular, eccentric annular, and tilted eccentric annular. The momentum flux profile was calculated assuming that Prandtl's 1/7 Power Law was valid near the pipe walls and along the axis perpendicular to the rake. Prandtl's Power Law was modified along the axis of the pitot tube rake to conform to the measured momentum fluxes. The equation used to characterize the momentum flux profile had several intuitively satisfying features. The equation was smooth, except for the inherent 1/7 Power Law cusp at the pipe center, passed exactly through all measured momentum fluxes, and followed a 1/7 Power Law for regions where no measured data are available. Equation (6) is the final form of the momentum flux profile equation.

$$\rho V^2(W,V) = \rho V^2_0(W)\left[1 - \left(\sqrt{W^2 + V^2}/R\right)\right]^{2/7} \qquad (6)$$

where

W = axis of pitot rake

V = axis perpendicular to pitot rake

R = pipe radius

$\rho V^2_0(W)$ = pipe center ρV^2 as a function of measured ρV^2.

Reference mass flow was computed from the output of four load cells. The data reduction equations used to produce mass flow from the load cell output are documented in Reference 5. Briefly, the system weight is determined using:

$$W_s = D_o + D_1 (E_1 + E_2 + E_3 + E_4) \qquad (7)$$

where

W_s = system weight

D_o, D_1 = calibration coefficients

$E_1 \ldots E_4$ = voltage output of load cells.

The resulting system weight is then low pass filtered and differentiated to provide an estimate of mass flow.

5. RESULTS

A total of 11 tests were conducted. For these tests, 5 had the PECC rake installed, 6 had the PDTT rake installed, 9 had the purge system on, 2 had the purge system off, and 1 was a single-phase test. Tables 3 through 13 give the mass flow calculated using the pitot tube rake, densitometer combination, the reference mass flow, and uncertainty in mass flow from the pitot tube rake. Two methods of calculating mass from the pitot tube rake are tabulated: rake axis symmetry and density axis symmetry. The only difference between the methods is the assumed axis of symmetry of the flow. (A more complete description is available in Reference 4.) The data in Tables 3 through 13 may be used to substantiate the following hypotheses:

1. The pitot tubes usually measure an integrated mass flow less than the reference mass flow

2. The rake axis symmetry model consistantly produces better estimates of integrated mass flow than the density axis model

3. There is no significant difference in mass flow estimation if a purge system is applied to the pitot tube sense lines

4. Kiel shields yielded no substantial improvement in the performance of the pitot tube rakes.

The integrated mass flow calculated using the rake axis symmetry from the pitot tubes had a mean value of 3.77 %RG (RG = range = 200 kg) below the reference; the density axis had a mean value of 23.10 %RG. Table 14 summarizes the %RG uncertainty at 45 s in the integrated mass flow and the estimated swirl in the flow. The time interval of 0 to 45 s was chosen because, essentially, all mass flow was over by 45 s in all of the tests. The cause of the consistent low readings is unknown; however, a postulated cause is the swirl present in the flow. Hutton[6] and Kinghorn[7] both comment on the effect of inlet swirl on flow meters. The conclusion of both researchers is that inlet swirl reduces the sensitivity of flow meters. A reduction in sensitivity of 0.2% on venturi meters has been seen, and higher reductions for other flow meters have been discussed. The data

TABLE 3. PDTT RAKE MASS FLOW (kg) FOR COLD SINGLE-PHASE TEST IB2SP01

Time Interval seconds	Rake Axis Symmetry	Density Axis Symmetry	Reference Mass Flow	Integral Rake Symmetry	Integral Density Symmetry	Integral Reference	Uncer. Rake Symmetry	Uncer. Density Symmetry	Uncer. Integral Rake	Uncer. Integral Densits
0- 5	817	839	228	817	839	228	257.99	267.54	257.99	267.54
5- 10	584	607	443	1401	1446	671	31.84	37.10	108.78	115.50
10- 15	475	475	419	1876	1921	1090	13.32	13.32	72.09	76.22
15- 20	428	428	415	2304	2349	1505	3.16	3.16	53.08	56.08
20- 25	404	404	303	2708	2753	1808	33.20	33.20	49.75	52.24
25- 30	319	326	330	3027	3079	2138	-3.27	-1.09	41.57	44.01
30- 35	200	283	412	3227	3362	2550	-51.47	-31.38	26.53	31.83
35- 40	131	173	106	3358	3535	2657	22.84	62.88	26.39	33.07
40- 45	58	60	25	3416	3595	2682	129.37	138.10	27.35	34.06

Note : Uncertainty is expressed as a %RD

TABLE 4. PDTT RAKE MASS FLOW (kg) FOR TEST IB201

Time Interval seconds	Rake Axis Symmetry	Density Axis Symmetry	Reference Mass Flow	Integral Rake Symmetry	Integral Density Symmetry	Integral Reference	Uncer. Rake Symmetry	Uncer. Density Symmetry	Uncer. Integral Rake	Uncer. Integral Density
0- 5	1076	1076	642	1076	1076	642	67.68	67.68	67.68	67.68
5- 10	833	833	665	1909	1909	1306	25.30	25.30	46.12	46.12
10- 15	581	581	595	2489	2489	1902	-2.47	-2.47	30.91	30.91
15- 20	498	498	581	2987	2987	2482	-14.30	-14.30	20.33	20.33
20- 25	296	296	355	3282	3282	2837	-16.69	-16.69	15.70	15.70
25- 30	127	127	179	3409	3409	3016	-29.07	-29.07	13.05	13.05
30- 35	67	67	-75	3476	3476	2940	-188.99	-188.99	18.23	18.23
35- 40	19	19	8	3495	3495	2948	134.18	134.18	18.54	18.54
40- 45	3	3	-25	3498	3498	2923	-111.31	-111.31	19.66	19.66

Note : Uncertainty is expressed as a %RD

TABLE 5. PDTT RAKE MASS FLOW (kg) FOR TEST IA201

Time Interval seconds	Rake Axis Symmetry	Density Axis Symmetry	Reference Mass Flow	Integral Rake Symmetry	Integral Density Symmetry	Integral Reference	Uncer. Rake Symmetry	Uncer. Density Symmetry	Uncer. Integral Rake	Uncer. Integral Density
0- 5	974	1060	961	974	1060	961	1.42	10.36	1.42	10.36
5- 10	867	1286	820	1842	2346	1780	5.83	56.89	3.45	31.78
10- 15	708	1100	692	2549	3446	2472	2.35	59.12	3.14	39.43
15- 20	548	853	603	3097	4299	3075	-9.26	41.35	0.71	39.81
20- 25	390	543	429	3487	4842	3504	-9.19	26.58	-0.50	38.19
25- 30	244	250	245	3731	5092	3749	-0.24	2.02	-0.49	35.83
30- 35	-46	-46	141	3685	5046	3889	-132.65	-132.65	-5.26	29.73
35- 40	-8	-8	57	3677	5038	3946	-114.43	-114.43	-6.83	27.67
40- 45	0	0	21	3677	5038	3967	-98.39	-98.39	-7.30	27.01
45- 50	-1	-1	23	3676	5037	3990	-105.28	-105.28	-7.87	26.24
50- 55	-3	-3	11	3673	5034	4000	-123.77	-123.77	-8.18	25.85
55- 60	-2	-2	16	3671	5033	4017	-110.91	-110.91	-8.60	25.29
60- 65	-6	-6	28	3665	5026	4045	-122.59	-122.59	-9.39	24.27
65- 70	-4	-4	23	3661	5023	4068	-116.13	-116.13	-9.99	23.47
70- 75	-3	-3	19	3658	5020	4087	-116.00	-116.00	-10.48	22.83
75- 80	-3	-3	16	3656	5017	4103	-116.39	-116.39	-10.90	22.28
80- 85	-1	-1	19	3655	5016	4122	-104.93	-104.93	-11.33	21.70
85- 90	2	2	11	3657	5018	4132	-81.29	-81.29	-11.51	21.43
90- 95	5	5	1	3661	5023	4133	483.89	483.89	-11.42	21.52
95-100	6	6	1	3667	5028	4134	855.94	855.94	-11.30	21.63
100-105	7	7	-2	3673	5035	4132	-529.73	-529.73	-11.10	21.84
105-110	7	7	-2	3681	5042	4130	-466.53	-466.53	-10.89	22.07
110-115	7	7	3	3688	5049	4133	179.98	179.98	-10.77	22.16

Note : Uncertainty is expressed as a %RD

TABLE 6. PDTT RAKE MASS FLOW (kg) FOR TEST 1A202

Time Interval seconds	Rake Axis Symmetry	Density Axis Symmetry	Reference Mass Flow	Integral Rake Symmetry	Integral Density Symmetry	Integral Reference	Uncer. Rake Symmetry	Uncer. Density Symmetry	Uncer. Integral Rake	Uncer. Integral Density
0- 5	1055	1276	868	1055	1276	868	21.57	46.93	21.57	46.93
5- 10	911	1284	823	1967	2560	1691	10.74	56.06	16.30	51.37
10- 15	665	959	696	2631	3519	2387	-4.49	37.84	10.24	47.43
15- 20	567	917	607	3198	4436	2994	-6.61	51.13	6.82	48.18
20- 25	343	427	370	3541	4864	3364	-7.44	15.33	5.25	44.56
25- 30	85	176	225	3626	5040	3590	-62.49	-21.93	1.00	40.39
30- 35	-57	-57	113	3568	4982	3703	-150.54	-150.54	-3.64	34.54
35- 40	-9	-9	34	3560	4973	3737	-126.08	-126.08	-4.75	33.09
40- 45	-1	-1	13	3559	4973	3750	-105.49	-105.49	-5.09	32.61
45- 50	-7	-7	9	3552	4966	3759	-171.96	-171.96	-5.50	32.12
50- 55	-4	-4	11	3548	4962	3769	-136.85	-136.85	-5.96	31.64
55- 60	-3	-3	19	3545	4959	3788	-116.12	-116.12	-6.41	30.92
60- 65	-1	-1	14	3544	4958	3802	-107.04	-107.04	-6.77	30.42
65- 70	1	1	16	3545	4959	3818	-93.63	-93.63	-7.14	29.89
70- 75	0	0	13	3545	4959	3831	-100.36	-100.36	-7.46	29.44
75- 80	1	1	21	3547	4960	3853	-94.35	-94.35	-7.95	28.75
80- 85	2	2	12	3549	4963	3865	-82.08	-82.08	-8.18	28.40
85- 90	3	3	18	3551	4965	3883	-85.58	-85.58	-8.54	27.87
90- 95	2	2	15	3554	4968	3898	-83.84	-83.84	-8.82	27.45
95-100	4	4	7	3558	4972	3905	-40.30	-40.30	-6.88	27.32
100-105	3	3	3	3561	4975	3908	1.68	1.68	-8.88	27.30
105-110	4	4	2	3565	4979	3910	81.02	81.02	-8.83	27.33
110-115	2	2	0	3567	4981	3910	551.66	551.66	-8.78	27.38

Note : Uncertainty is expressed as a %RD

TABLE 7. PDTT RAKE MASS FLOW (kg) FOR TEST IIA201

Time Interval seconds	Rake Axis Symmetry	Density Axis Symmetry	Reference Mass Flow	Integral Rake Symmetry	Integral Density Symmetry	Integral Reference	Uncer. Rake Symmetry	Uncer. Density Symmetry	Uncer. Integral Rake	Uncer. Integral Density
0- 5	309	411	363	309	411	363	-14.83	13.34	-14.83	13.34
5- 10	268	378	310	577	789	673	-13.65	22.05	-14.29	17.35
10- 15	217	306	274	794	1095	947	-20.83	11.53	-16.18	15.66
15- 20	230	325	258	1023	1420	1204	-10.72	26.14	-15.01	17.90
20- 25	230	325	250	1254	1745	1454	-7.77	30.37	-13.77	20.04
25- 30	174	248	201	1428	1993	1655	-13.15	23.46	-13.70	20.46
30- 35	159	227	154	1587	2220	1809	2.92	47.50	-12.28	22.76
35- 40	146	209	135	1733	2429	1944	8.22	54.63	-10.86	24.98
40- 45	130	185	109	1863	2614	2053	19.17	69.36	-9.26	27.33
45- 50	95	127	89	1957	2741	2142	6.17	42.38	-8.62	27.96
50- 55	49	50	87	2007	2791	2229	-43.22	-42.64	-9.97	25.20
55- 60	36	36	59	2043	2827	2288	-38.27	-38.10	-10.70	23.58
60- 65	28	28	52	2071	2855	2340	-46.93	-46.93	-11.50	22.00
65- 70	23	23	50	2094	2878	2390	-52.93	-52.93	-12.36	20.45
70- 75	20	20	17	2114	2898	2407	15.52	15.52	-12.16	20.42
75- 80	15	15	46	2129	2914	2453	-67.24	-67.24	-13.20	18.76
80- 85	12	12	24	2141	2925	2477	-50.85	-50.85	-13.56	18.10
85- 90	10	10	16	2151	2935	2493	-40.74	-40.74	-13.74	17.71
90- 95	8	8	26	2159	2943	2519	-69.11	-69.11	-14.31	16.82
95-100	6	6	24	2165	2949	2543	-74.15	-74.15	-14.86	15.98
100-105	5	5	21	2170	2954	2564	-75.83	-75.83	-15.36	15.22
105-110	4	4	18	2174	2958	2581	-77.14	-77.14	-15.78	14.59
110-115	3	3	17	2177	2961	2598	-80.84	-80.84	-16.20	13.98
115-120	3	3	14	2180	2964	2612	-81.69	-81.69	-16.56	13.46

Note : Uncertainty is expressed as a %RD

TABLE 8. PDTT RAKE MASS FLOW (kg) FOR TEST IIA202

Time Interval seconds	Rake Axis Symmetry	Density Axis Symmetry	Reference Mass Flow	Integral Rake Symmetry	Integral Density Symmetry	Integral Reference	Uncer. Rake Symmetry	Uncer. Density Symmetry	Uncer. Integral Rake	Uncer. Integral Density
0- 5	340	450	370	340	450	370	-8.13	21.63	-8.13	21.63
5- 10	291	412	286	632	862	657	1.75	43.87	-3.82	31.33
10- 15	247	348	266	879	1211	923	-7.14	30.94	-4.78	31.22
15- 20	240	340	254	1119	1550	1177	-5.51	33.63	-4.94	31.74
20- 25	243	343	249	1361	1893	1426	-2.49	37.88	-4.51	32.81
25- 30	192	274	207	1554	2167	1632	-6.83	32.45	-4.80	32.76
30- 35	177	253	158	1730	2419	1790	11.98	60.14	-3.32	35.18
35- 40	160	227	134	1890	2647	1924	19.19	69.83	-1.76	37.59
40- 45	135	190	123	2025	2837	2046	10.45	55.43	-1.03	38.66
45- 50	96	121	98	2121	2959	2145	-2.85	23.27	-1.11	37.95
50- 55	56	56	82	2177	3015	2227	-31.91	-31.30	-2.25	35.40
55- 60	47	47	67	2224	3062	2294	-30.25	-30.10	-3.06	33.48
60- 65	40	40	55	2264	3102	2349	-26.86	-26.86	-3.62	32.07
65- 70	34	34	64	2298	3136	2413	-46.87	-46.87	-4.77	29.98
70- 75	28	28	28	2325	3164	2441	-1.78	-1.78	-4.73	29.61
75- 80	23	23	26	2349	3187	2467	-11.07	-11.07	-4.80	29.18
80- 85	21	21	28	2370	3208	2495	-23.74	-23.74	-5.01	28.59
85- 90	20	20	18	2389	3228	2513	6.56	6.56	-4.93	28.43
90- 95	19	19	13	2409	3247	2526	51.18	51.18	-4.64	28.55
95-100	17	17	17	2425	3263	2543	-4.05	-4.05	-4.64	28.32
100-105	17	17	16	2442	3280	2559	4.93	4.93	-4.58	28.18
105-110	17	17	10	2459	3297	2570	61.54	61.54	-4.31	28.31
110-115	16	16	15	2475	3313	2584	8.16	8.16	-4.24	28.20
115-120	17	17	15	2491	3330	2599	11.33	11.33	-4.15	28.10

Note : Uncertainty is expressed as a %RD

TABLE 9. PECC RAKE MASS FLOW (kg) FOR TEST IIIA101

Time Interval seconds	Rake Axis Symmetry	Density Axis Symmetry	Reference Mass Flow	Integral Rake Symmetry	Integral Density Symmetry	Integral Reference	Uncer. Rake Symmetry	Uncer. Density Symmetry	Uncer. Integral Rake	Uncer. Integral Density
0- 5	1003	1066	912	1003	1066	912	10.00	16.90	10.00	16.90
5- 10	850	1146	867	1854	2212	1779	-1.95	32.14	4.18	24.33
10- 15	682	988	722	2535	3200	2502	-5.61	36.80	1.35	27.93
15- 20	526	769	656	3061	3970	3158	-19.88	17.27	-3.06	25.72
20- 25	265	295	406	3326	4265	3564	-34.64	-27.26	-6.66	19.68
25- 30	121	121	198	3447	4386	3762	-39.03	-39.03	-8.36	16.59
30- 35	92	92	119	3539	4477	3880	-22.76	-22.76	-8.80	15.39
35- 40	36	36	61	3574	4513	3941	-41.50	-41.50	-9.31	14.51
40- 45	4	4	12	3579	4517	3953	-65.65	-65.65	-9.48	14.28

TABLE 10. PECC RAKE MASS FLOW (kg) FOR TEST IIIA102

Time Interval seconds	Rake Axis Symmetry	Density Axis Symmetry	Reference Mass Flow	Integral Rake Symmetry	Integral Density Symmetry	Integral Reference	Uncer. Rake Symmetry	Uncer. Density Symmetry	Uncer. Integral Rake	Uncer. Integral Density
0- 5	972	990	955	972	990	955	1.82	3.73	1.82	3.73
5- 10	841	1190	872	1813	2180	1827	-3.55	36.43	-0.75	19.34
10- 15	704	1199	732	2517	3379	2559	-3.85	63.77	-1.63	32.05
15- 20	611	1061	649	3128	4439	3208	-5.85	63.35	-2.49	38.38
20- 25	336	436	395	3464	4875	3603	-15.13	10.19	-3.87	35.29
25- 30	129	129	167	3593	5004	3771	-22.64	-22.62	-4.71	32.72
30- 35	77	77	90	3670	5082	3860	-13.72	-13.73	-4.92	31.64
35- 40	42	42	58	3712	5123	3918	-28.32	-28.32	-5.26	30.76
40- 45	19	19	31	3731	5142	3949	-39.56	-39.56	-5.53	30.21

Note : Uncertainty is expressed as a %RD

TABLE 11. PECC RAKE MASS FLOW (kg) FOR TEST IIIA201

Time Interval seconds	Rake Axis Symmetry	Density Axis Symmetry	Reference Mass Flow	Integral Rake Symmetry	Integral Density Symmetry	Integral Reference	Uncer. Rake Symmetry	Uncer. Density Symmetry	Uncer. Integral Rake	Uncer. Integral Density
0- 5	1102	1210	953	1102	1210	953	15.67	27.02	15.67	27.02
5- 10	905	1320	939	2007	2530	1891	-3.58	40.67	6.11	33.79
10- 15	672	1062	748	2679	3593	2639	-10.08	42.03	1.52	35.13
15- 20	529	803	636	3209	4395	3275	-16.76	26.18	-2.03	34.20
20- 25	234	243	350	3443	4638	3626	-33.17	-30.75	-5.04	27.92
25- 30	97	97	139	3540	4735	3764	-30.30	-30.30	-5.97	25.77
30- 35	66	66	86	3606	4801	3850	-22.84	-22.84	-6.34	24.69
35- 40	25	25	47	3631	4826	3897	-46.99	-46.99	-6.83	23.83
40- 45	3	3	20	3634	4829	3917	-84.39	-84.39	-7.23	23.27

TABLE 12. PECC RAKE MASS FLOW (kg) FOR TEST IIIA202

Time Interval seconds	Rake Axis Symmetry	Density Axis Symmetry	Reference Mass Flow	Integral Rake Symmetry	Integral Density Symmetry	Integral Reference	Uncer. Rake Symmetry	Uncer. Density Symmetry	Uncer. Integral Rake	Uncer. Integral Density
0- 5	1029	1075	952	1029	1075	952	8.05	12.83	8.05	12.83
5- 10	888	1277	887	1917	2351	1840	0.04	43.88	4.19	27.80
10- 15	686	1055	743	2602	3406	2583	-7.74	41.95	0.76	31.88
15- 20	550	863	652	3152	4269	3235	-15.64	32.34	-2.55	31.97
20- 25	317	388	391	3469	4657	3626	-18.94	-0.75	-4.32	28.44
25- 30	127	127	170	3596	4784	3796	-25.58	-25.58	-5.27	26.02
30- 35	85	85	95	3681	4869	3891	-10.96	-10.95	-5.41	25.11
35- 40	44	44	57	3725	4913	3948	-22.24	-22.24	-5.65	24.43
40- 45	17	17	28	3742	4930	3976	-39.18	-39.18	-5.89	23.98

Note : Uncertainty is expressed as a %RD

TABLE 13. PECC RAKE MASS FLOW (kg) FOR TEST IVA101

Time Interval seconds	Rake Axis Symmetry	Density Axis Symmetry	Reference Mass Flow	Integral Rake Symmetry	Integral Density Symmetry	Integral Reference	Uncer. Rake Symmetry	Uncer. Density Symmetry	Uncer. Integral Rake	Uncer. Integral Density
0- 5	478	478	505	478	478	505	-5.25	-5.24	-5.25	-5.24
5- 10	364	363	406	842	841	911	-10.52	-10.74	-7.60	-7.69
10- 15	275	277	340	1116	1118	1251	-19.33	-18.75	-10.79	-10.70
15- 20	320	333	324	1436	1450	1575	-1.11	2.83	-8.80	-7.92
20- 25	297	311	301	1734	1761	1876	-1.03	3.47	-7.56	-6.09
25- 30	274	283	285	2007	2044	2160	-3.84	-0.64	-7.07	-5.38
30- 35	247	253	270	2254	2297	2430	-8.64	-6.48	-7.24	-5.56
35- 40	223	229	244	2478	2526	2675	-8.63	-6.22	-7.37	-5.56
40- 45	200	214	247	2677	2740	2922	-19.25	-13.51	-8.38	-6.24
45- 50	148	173	210	2826	2913	3133	-29.49	-17.95	-9.79	-7.02
50- 55	70	95	145	2895	3008	3277	-51.94	-34.10	-11.65	-8.22
55- 60	67	74	110	2962	3082	3387	-39.18	-32.63	-12.55	-9.01
60- 65	54	55	64	3016	3137	3451	-16.04	-14.69	-12.61	-9.12
65- 70	44	44	58	3061	3181	3510	-23.90	-23.90	-12.80	-9.36
70- 75	36	36	36	3097	3218	3546	-0.14	-0.14	-12.67	-9.27

Note : Uncertainty is expressed as a %RD

presented in Table 14 is generally consistent with the hypothesis that swirl effects reduce the sensitivity of the pitot tubes; however, the estimated swirl factor was highly subjective and, consequently, quite open to dispute. A more complete data base, including direct swirl measurements will be necessary before any substantive conclusions may be drawn.

The reduction in sensitivity was also postulated to be an effect of fluid density, pressure, or pressure drop across the measurement port. These hypotheses were tested by attempting to define a polynomial which could correlate density, pressure, or pressure drop with the measured uncertainty. Figures 12 through 19 show the results of these attempts, none were in the least successful.

The second problem investigated was the effect of a purge system on the pitot rake performance. Two pairs of tests were conducted with and without purge water: IA201 and IA202, and IIIA201 and IIIA202. Table 15 shows no meaningful correlation between purge system status and the effectiveness of the pitot tubes as mass flow measuring devices. It should be noted that this conclusion is based on a very limited data set and is, therefore, of dubious value.

The third bit of information we wished to derive from this test data was the effect of Kiel shields on pitot tube performance. The data in Tables 3 through 14 clearly show that the Kiel shields produced no significant increase or decrease in the estimated uncertainty in mass flow. Kiel shields are designed to reduce the effect of tangential components in the flow field. Hence, without an accurate knowledge of these tangential flows, it is not possible to determine whether the Kiel shields were not effective or significant tangential flows simply did not exist.

TABLE 14. UNCERTAINTY IN INTEGRATED MASS FLOW VERSUS SWIRL

Test	Rake Type	Swirl Factor[a]	Uncertainty at 45 s
IB2SP01	PDTT	1	27.35
IB201	PDTT	5	19.66
IIA202	PDTT	5	-1.03
IA202	PDTT	9	-5.09
IIIA102	PECC	10	-5.53
IIIA202	PECC	10	-5.89
IVA101	PECC	6	-6.24
IIIA201	PECC	10	-7.23
IA201	PDTT	9	-7.30
IIA201	PDTT	5	-9.26
IIIA101	PECC	10	-9.48

a. Swirl factor = (orifice size = 2) + 2 x (orifice = 4) + 3x (orifice >4) + (elbow installed) x 4 + (downcomer installed) x 2 + (nozzle not installed).

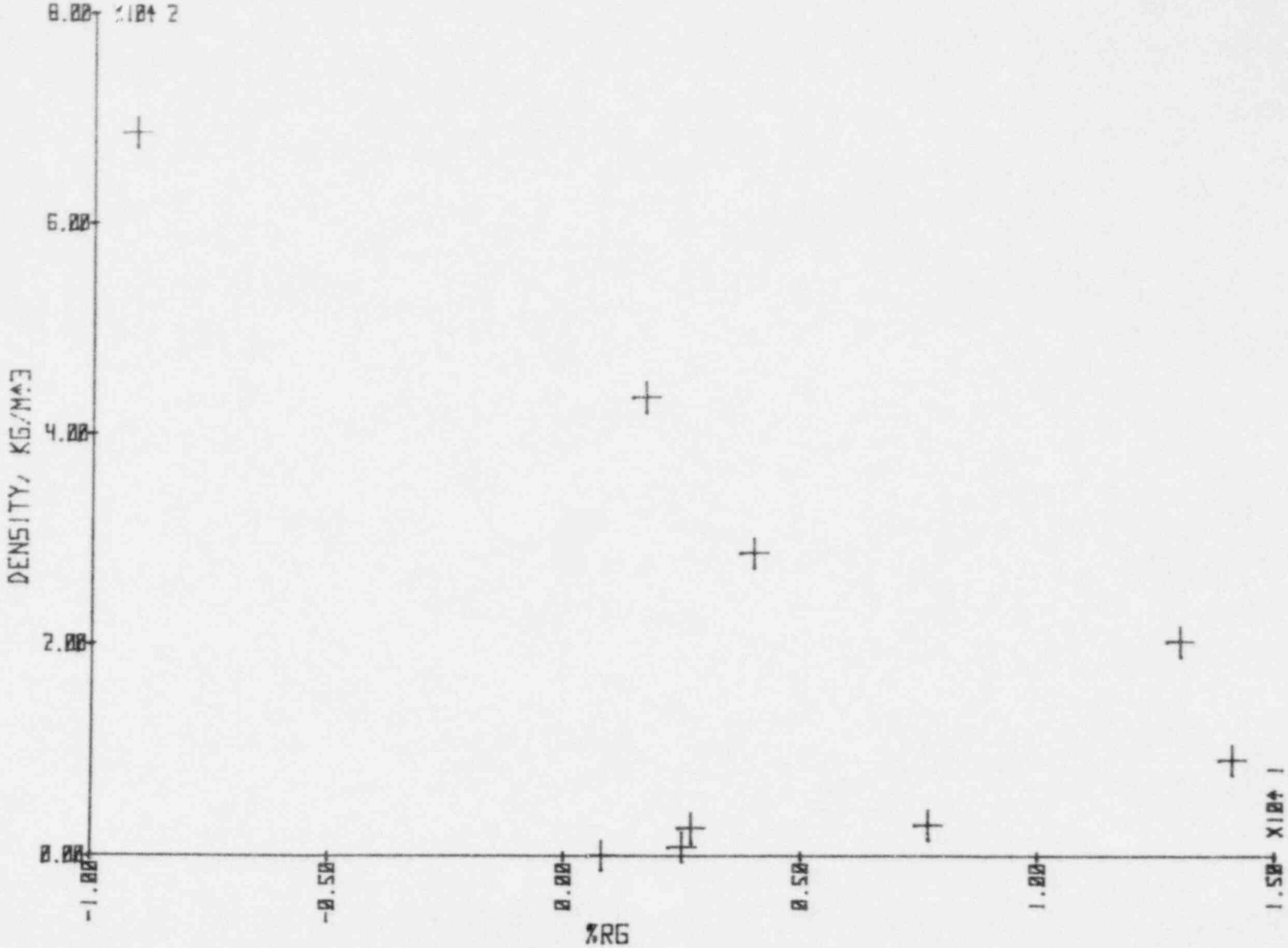

Figure 12. Wyle differential rake %RG versus density for Test IIIA101.

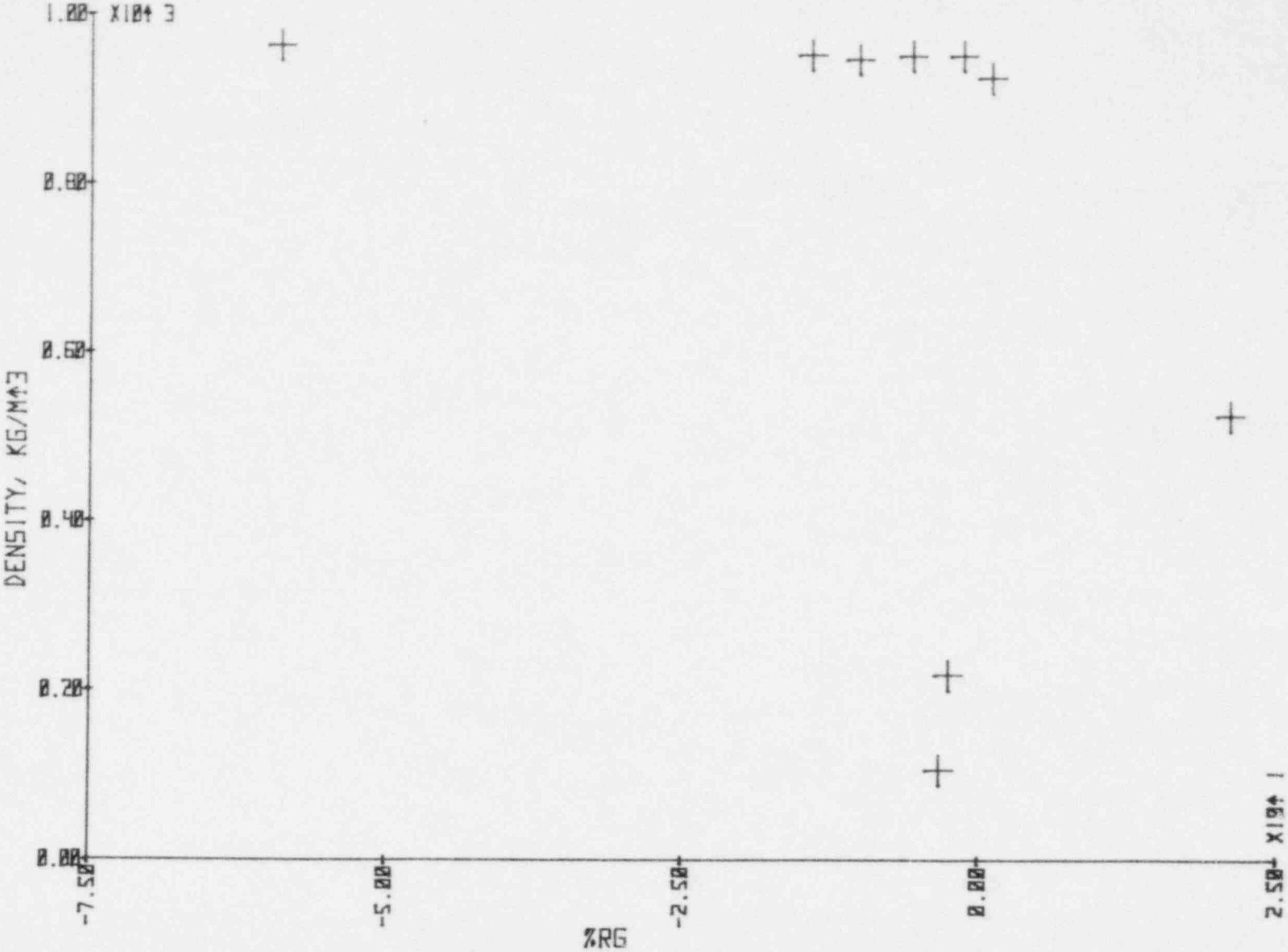

Figure 13. Wyle differential rake %RG versus density for Test IB2SP01.

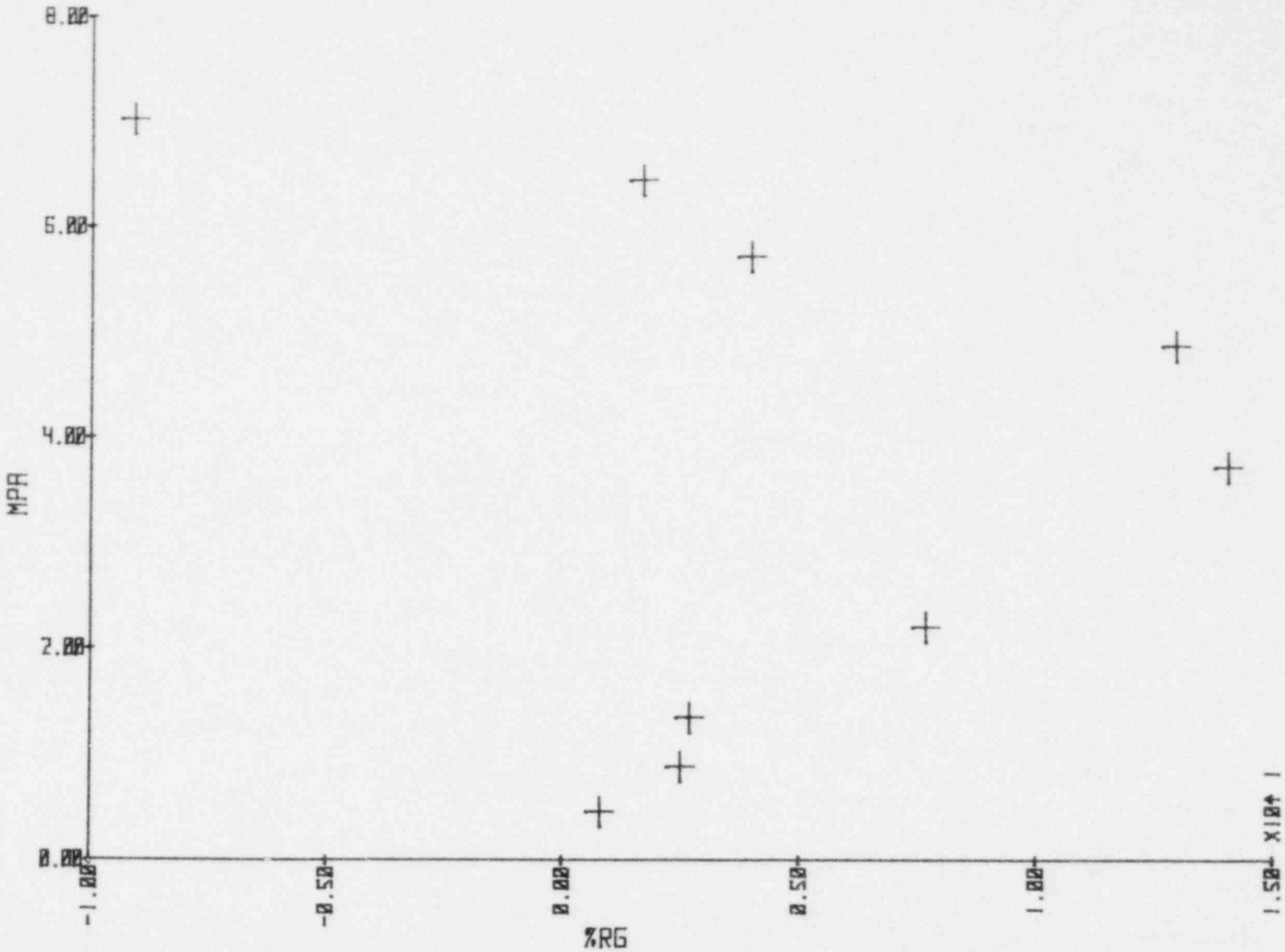

Figure 14. Wyle differential rake %RG versus pressure at P-SP2-1 for Test IIIA101.

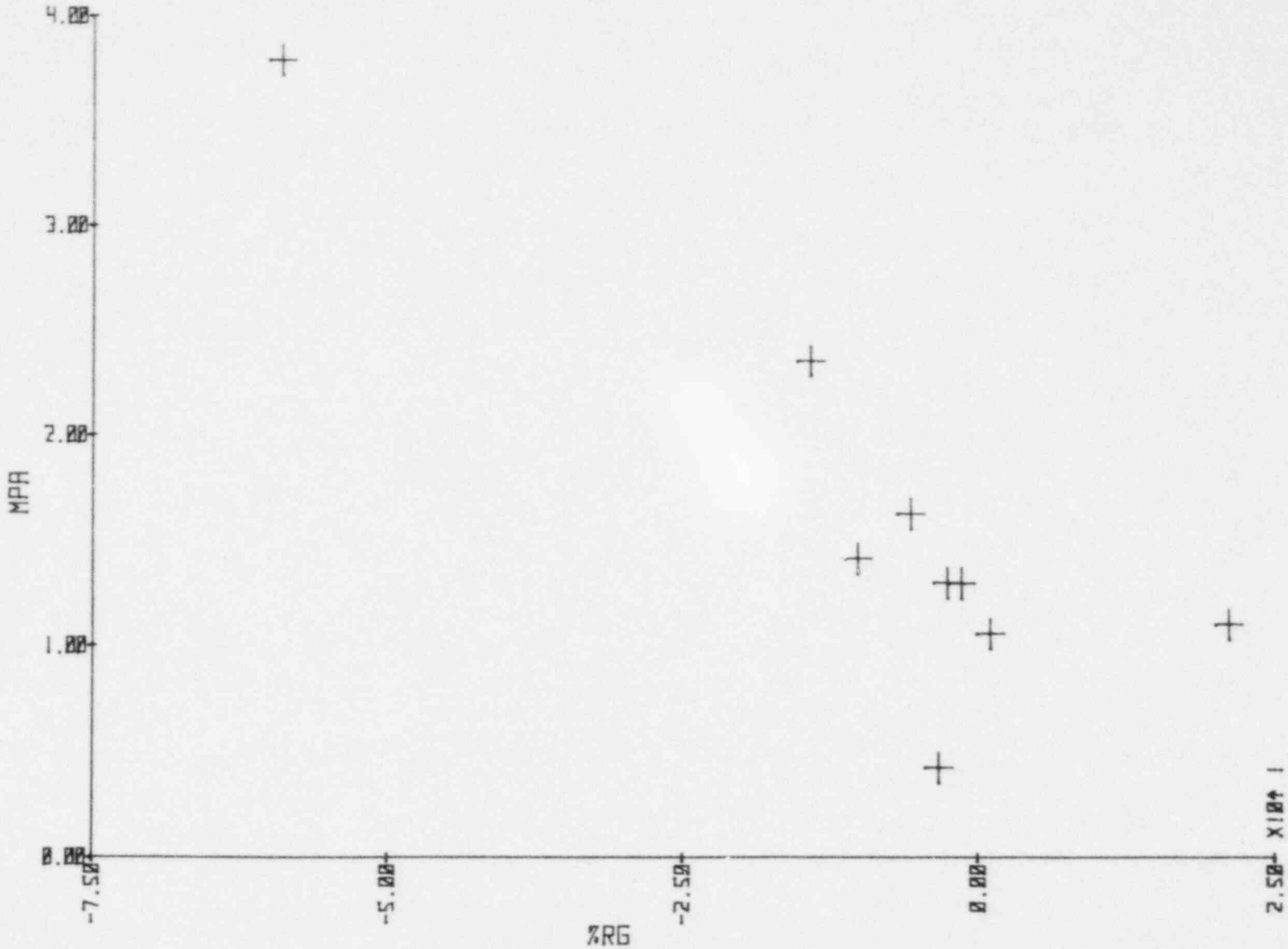

Figure 15. Wyle differential rake %RG versus pressure at P-SP2-1 for Test IB2SP01.

LTR LO-87-80-142

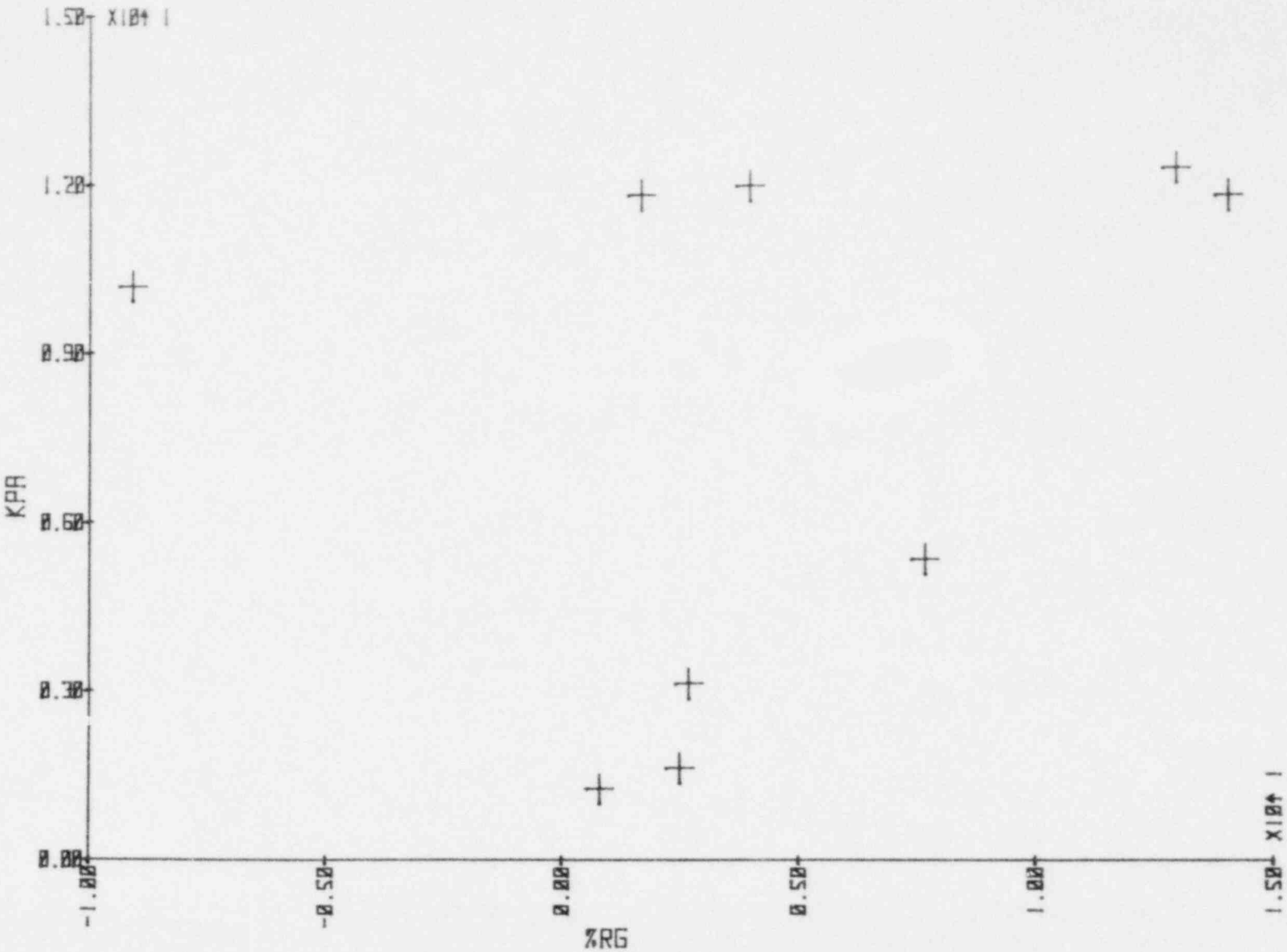

Figure 16. Wyle differential rake %RG versus differential pressure at DP-SP2-1 for Test IIIA101.

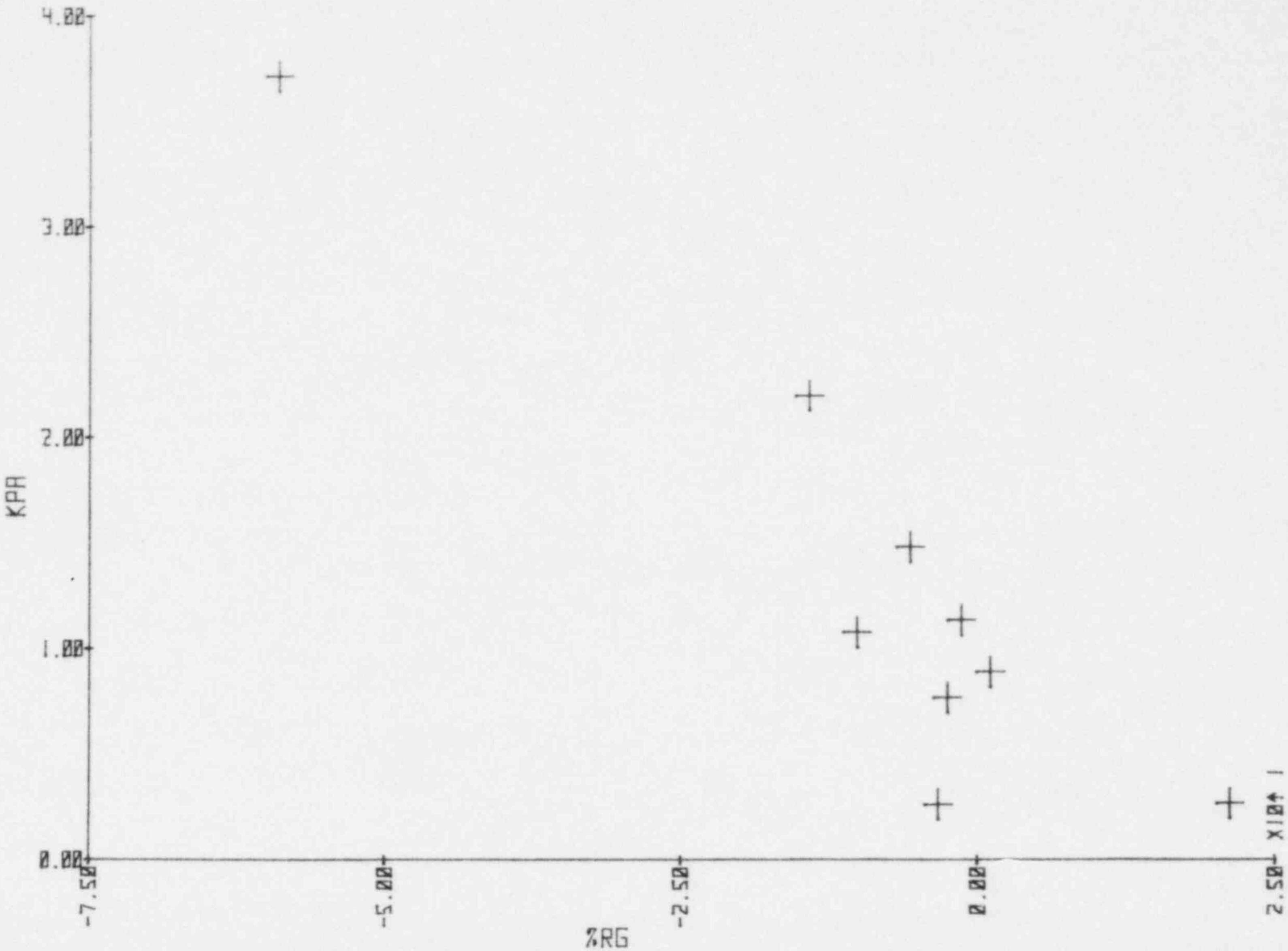

Figure 17. Wyle differential rake %RG versus differential pressure at DP-SP2-1 for Test IB2SP01.

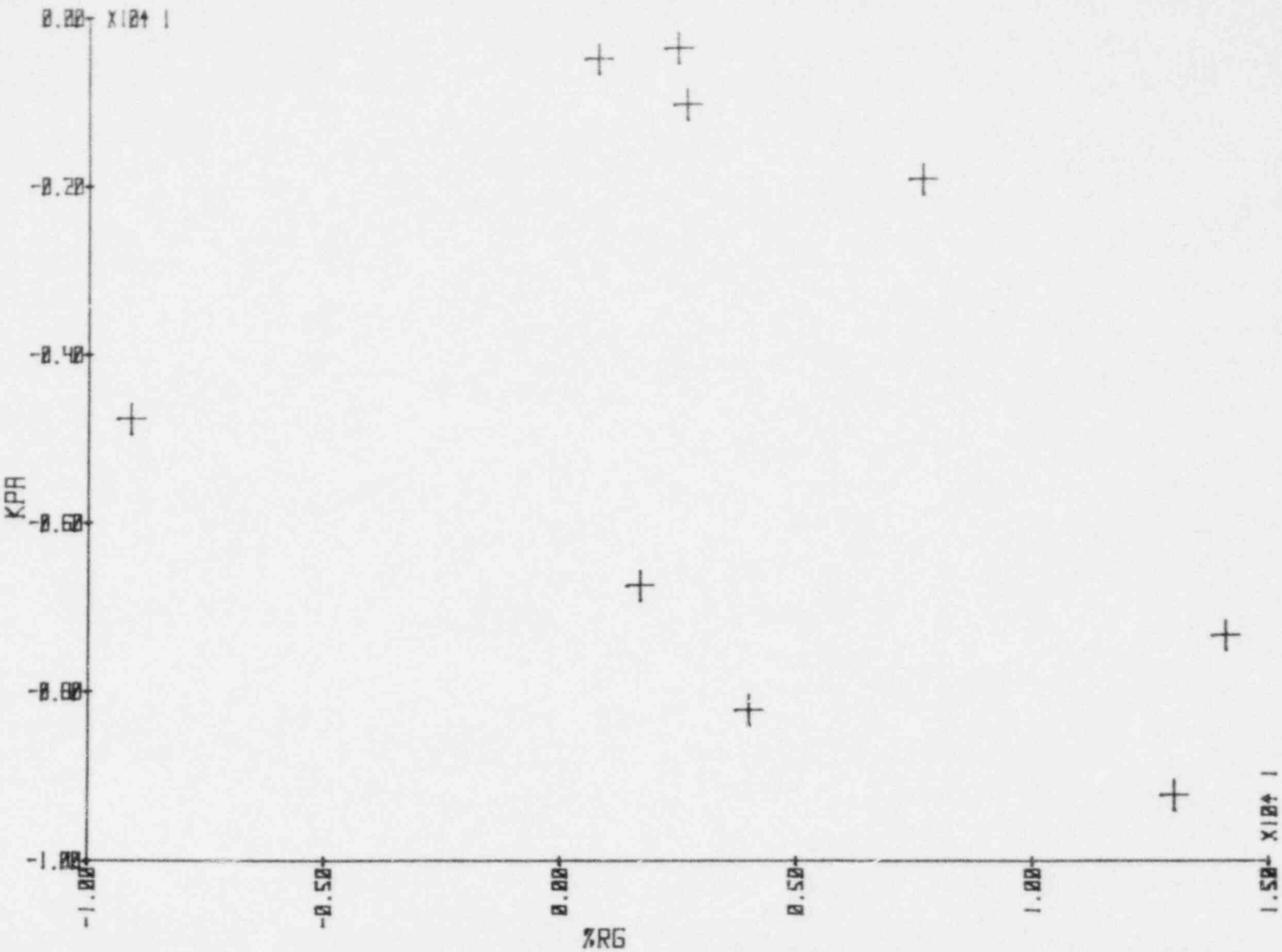

Figure 18. Wyle differential rake %RG versus differential pressure at DP-SP2-2 for Test IIIA1C1.

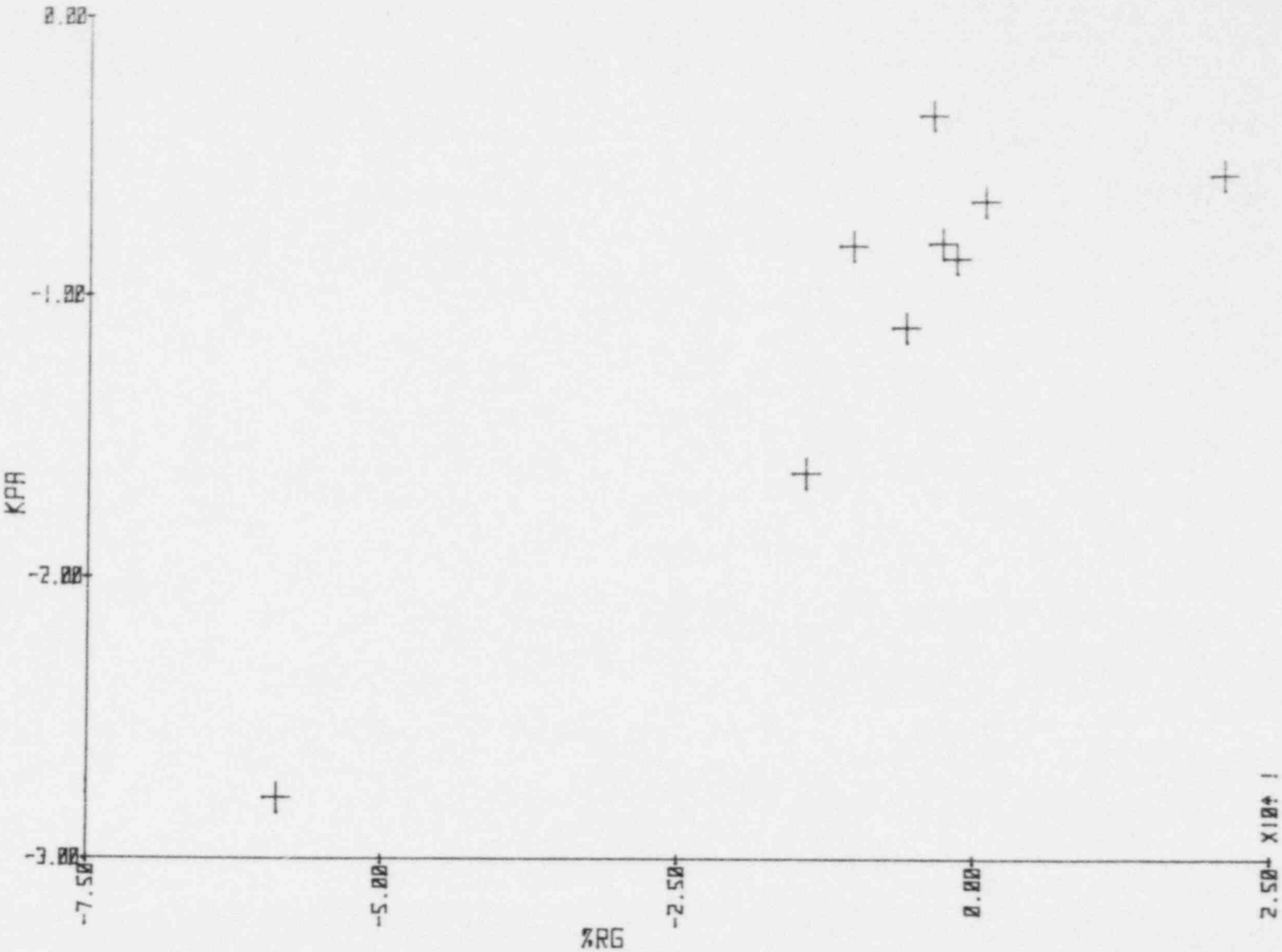

Figure 19. Wyle differential rake %RG versus differential pressure at DP-SP2-2 for Test IB2SP01.

TABLE 15. THE PURGE SYSTEM EFFECT ON UNCERTAINTY IN MASS FLOW (%RD UNCERTAINTY IN MASS FLOW)

Time (s)	Water Off (Test IA201)	Water On (Test IA202)	Water Off (Test IIIA201)	Water On (Test IIIA202)
0 to 5	1.42	21.57	15.67	8.05
5 to 10	5.83	10.74	-3.58	0.04
10 to 15	2.35	-4.49	-10.08	-7.74
15 to 20	-9.26	-6.61	-16.76	15.64
20 to 25	-9.19	-7.44	-33.17	-18.94
25 to 30	-0.24	-62.49	-30.30	-25.58
30 to 35	-132.65	-150.54	-22.84	-10.96
35 to 40	-114.43	-126.08	-46.99	-22.24
40 to 45	-98.39	-105.08	-84.39	-39.18

6. CONCLUSIONS

Pitot tubes in conjunction with density measuring devices and analytic models have been shown to produce acceptable estimates of mass flow during transient two-phase conditions. The uncertainty in mass flow may eventually be as good as ± 1.89 %RG; however, significant work remains prior to achieving an uncertainty this low. The LTCF tests have pinpointed the areas in which effort should be expended to achieve the lowest possible uncertainty. The areas which require work are: (a) the cause of the bias of -1.87 %RG, (b) the effects of swirl and Kiel shields on pitot tube performance, and (c) a more repeatable instrument configuration. The LTCF tests also showed those areas where work is not necessary. The analytic models tested indicated that the rake axis model was clearly superior. The effects of a continuous purge system are probably negligible and, hence, should not be required for future tests.

7. REFERENCES

1. J. R. Fincke and V. A. Deason, "Mass Flow Rate Measurements in Two-Phase Mixtures with Stagnation Probes," International Colloquium on Two-Phase Flow Instrumentation, Idaho Falls, Idaho, June 1979.

2. D. L. Reeder, LOFT System and Test Description (5.5 ft Nuclear Core 1 LOCEs), NUREG/CR-0247, TREE-1208, July 1978.

3. J. L. Wambach et al., Experimental Data Report for Transient Flow Calibration Facility Tests IIA101, IIA102, IIA201, and IIA202, LO-00-80-119, March 1980.

4. Letter: G. D. Lassahn to L. D. Goodrich, "User Manual for DPROF3 and EMDOT3," GDL-3-79, July 1979.

5. R. Good and T. R. Meacham, Analysis of a Transient Load Measuring System, LO-87-80-132, March 1980.

6. S. P. Hutton, "The Effect of Inlet Flow Conditions on the Accuracy of Flowmeter," Presented at Conference on Component Interactions in Fluid Flow Systems, March 7, 1974. Sponsored By: Thermodynamics and Fluid Mechanics Group of the Institution of Mechanical Engineers.

7. F. C. Kinghorn, "The On-Site Calibration of a Large Pressure Difference Flowmeter in Difficult Flow Conditions," Presented at Conference on Component Interactions in Fluid Flow Systems, March 7, 1974. Sponsored By: Thermodynamics and Fluid Mechanics Group of the Institution of Mechanical Engineers.